

HETEROGENEOUS PHOTOCATALYTIC REMOVAL
OF GASEOUS DILUTE BENZENE STREAMS
VIA NEAR ULTRAVIOLET ILLUMINATED
TITANIUM DIOXIDE

BY

LAWRENCE JOHN DEFLURI

Bachelor of Science

Pennsylvania State University

University Park, Pennsylvania

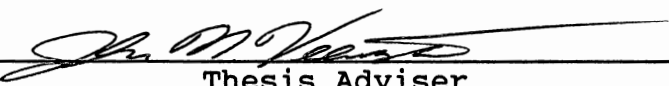
1986

Submitted to the Faculty of the
Graduate College of the
Oklahoma State University
in partial fulfillment of
the requirements for
the Degree of
MASTER OF SCIENCE
December, 1992

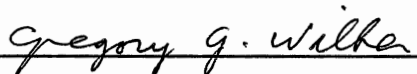
Thesis
1992
D313f.

HETEROGENEOUS PHOTOCATALYTIC REMOVAL
OF GASEOUS DILUTE BENZENE STREAMS
VIA NEAR ULTRAVIOLET ILLUMINATED
TITANIUM DIOXIDE

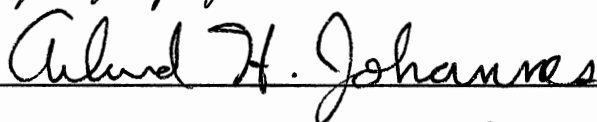
Thesis Approved:




Thesis Adviser



Gregory G. Wilber



Alward H. Johannes



Dean of the Graduate College

ACKNOWLEDGMENTS

There are a number of individuals who deserve recognition for their contributions in this successful research endeavor. First and foremost on the list is my wife Elizabeth. Her never ending encouragement, compassion and understanding helped me through every day at Oklahoma State. I realize that none of this could have been possible without her by my side.

I would also like to thank my major research advisor Dr. John Veenstra. His superior guidance and advisement throughout every phase of this project is greatly appreciated. Likewise I would like to extend my sincere gratitude to Dr. Greg Wilber and Dr. A. J. Johannas for their contributions as committee members. I counted on both of them for their insight and consultation on many key issues of this research and I am grateful for their time and effort.

My parents also deserve recognition for their love and twenty-eight years of constant encouragement. Beth's parents also provided us with much support and love and I am deeply grateful for both of them.

Special thanks are due to my friends Steven Katsinas and Cathy Southwick. I enjoyed their company in Stillwater and am grateful for their advise and friendship.

TABLE OF CONTENTS

| Chapter | Page |
|--|------|
| I. INTRODUCTION. | 1 |
| Benzene. | 3 |
| Physicochemical & Toxicological Properties. | 4 |
| Emission Standards | 5 |
| Benzene Treatment Options | 6 |
| Conventional Water Treatment | 6 |
| Oxidation and Ultraviolet Irradiation. | 6 |
| Aeration | 7 |
| Research Goals. | 9 |
| II. LITERATURE REVIEW | 10 |
| Photochemical Principals | 11 |
| Titanium Dioxide-Semiconductor Properties | 12 |
| Photocatalytic Research Involving Liquid Phase Organics | 16 |
| Photocatalytic Research Involving Gaseous Phase Organics. | 19 |
| III. METHODS AND MATERIALS | 24 |
| Experimental Apparatus | 24 |
| Fluidized-Bed Reactor. | 26 |
| Catalyst Preparation | 29 |
| Experimental Techniques. | 31 |
| IV. RESULTS AND DISCUSSION. | 33 |
| Results. | 36 |
| Discussion | 59 |
| V. SUMMARY AND RECOMMENDATIONS | 68 |
| Recommendations. | 71 |

LIST OF TABLES

| Table | Page |
|--|------|
| I. Volatile Organic Compounds Found In Ground Water Used For Drinking | 2 |
| II. Catalyst Bed Properties | 29 |
| III. Experimental Operating Parameters | 33 |
| IV. Experimental Reaction Rates | 34 |
| V. Photocatalytic Activation Rates | 36 |

LIST OF FIGURES

| Figure | Page |
|--|------|
| 1. Experimental Apparatus | 24 |
| 2. Fluidized-Bed Reactor | 27 |
| 3. Results of Experiment #1 | 38 |
| 4. Results of Experiment #2 | 39 |
| 5. Results of Experiment #3 | 40 |
| 6. Results of Experiment #4 | 41 |
| 7. Results of Experiment #5 | 42 |
| 8. Results of Experiment #6 | 43 |
| 9. Results of Experiments #7, #7A, #7B, & #7C | 44 |
| 10. Results of Experiments #8, #8A, #8B, & #8C | 45 |
| 11. Results of Experiments #9, #9A, & #9B | 46 |
| 12. Results of Experiments #10 & 10A | 47 |
| 13. Results of Experiment #11 | 48 |
| 14. Results of Experiments #12 & #12A | 49 |
| 15. Results of Experiment #13 | 50 |
| 16. Results of Experiment #14 | 51 |
| 17. Results of Experiments #15 & #15A | 52 |
| 18. Results of Experiment #16 | 54 |
| 19. Continuation of Experiment #16 | 55 |
| 20. Results of Experiment #17 | 57 |

| Figure | Page |
|--|------|
| 21. Continuation of Experiment #17 | 58 |
| 22. Photocatalytic Activation Time vs. Relative Humidity | 60 |
| 23. Removal Efficiency vs. Q_R | 61 |
| 24. Removal Efficiency vs. Relative Humidity | 62 |
| 25. R_G vs. Concentration | 64 |
| 26. R_G vs. Relative Humidity | 65 |
| 27. R_G vs. Q_R | 67 |

CHAPTER I

INTRODUCTION

Environmental initiatives have placed an ever increasing amount of pressure on the control of volatile organic compounds. Given the seemingly endless number of industrial and commercial sources which emit VOC emissions, a tremendous amount of research has been focused on technology which aims to reduce or eliminate such emissions. Photo-assisted catalytic decomposition has evolved as a promising area in VOC emission research.

Few concerns facing the environment have attracted as much attention in recent years as the pollution of ground water supplies. A major contributing effect of this pollution stems from the thousands of leaking gasoline storage tanks which have been discovered throughout the United States. Gasoline is a mixture of dozens of hydrocarbon compounds generally having molecular weights below 150. Benzene is the most water soluble component of gasoline and typically represents 2% to 5% of the total weight (Hadley, 1991). Benzene, which is quite volatile, (due to it's high vapor pressure) is listed by the EPA as a hazardous air pollutant (42 ^oFR, 1977), and as a VOC which has been found throughout the U.S. in groundwaters used for

public drinking water supplies (EPA, 1985). Please refer to Table I below.

TABLE I
VOLATILE ORGANIC COMPOUNDS FOUND IN GROUND WATER
USED FOR DRINKING (Westrick, 1984)

| | |
|-----------------------------|-----------------------|
| trichloroethylene* | benzene++ |
| tetrachloroethylene* | chlorobenzene++ |
| carbon tetrachloride+ | dichlorobenzene(s)++ |
| 1,1,1-trichloromethane+ | 1,1-dichloroethylene* |
| vinyl chloride* | 1,2-dichloroethane+ |
| cis-1,2-dichloroethylene* | methylene chloride+ |
| trans-1,2-dichloroethylene* | trichlorobenzene(s)++ |

*alkene (unsaturated compound)
+alkane (saturated compound)
++aromatic

Remediation of VOC contaminated groundwater is frequently performed by air stripping, a process that transfers the contaminants from the water phase to the air phase by contacting the phases counter-currently through a packed-bed column. Although air stripping has proven to be effective and economical for removing VOC's from groundwater, many states now require the use of an off-gas emissions control device in addition to the aeration unit. Typically these devices consist of a catalytic or thermal

incinerator unit. Given the two choices, a catalytic unit would be expected to be more economical since it usually operates at a lower temperature to obtain equivalent destruction efficiencies.

Recent studies have suggested that gas-solid heterogeneous photocatalytic oxidation of VOC's may be achieved using a fluidized-bed reactor system employing near ultraviolet illuminated TiO_2 . The objective of this research is to examine the potential contributions a fluidized-bed photocatalytic reactor may have in controlling dilute gaseous benzene emissions.

Benzene

Benzene is a carcinogenic, flammable, toxic, clear, colorless, volatile liquid with a familiar aromatic odor. It is used as a solvent for rubber and other polymeric materials and it replaced tetraethyl lead as an additive in unleaded gasoline. It is also an intermediate or raw material in the manufacture of detergents, dyes, explosives, pesticides, plastics and many other chemicals. It is amongst the 20 highest chemicals in volume produced in the United States (Fire, 1988). However, a push toward cleaner-burning fuels as mandated under the 1990 Clean Air Act Amendments (CAAA) could drastically reduce the amount of benzene and other aromatics in gasoline. The CAAA will require the refiners to reformulate gasoline blends in nine of the nation's worst ozone non-attainment areas by the year

1995. These reformulated blends are to limit total benzene content to less than or equal to 1 % volume. The current benzene average is approximately 2 % volume. It is estimated that between 25-30% of the total gasoline pool (7.2 million bbl/d in 1991) will be affected by these regulations (Shearman, 1992).

Physicochemical & Toxicological

Properties.

Benzene is the simplest of the class of organic chemicals known as "aromatic." It earned this name when it was first synthesized as the odor was described as being pleasant and aromatic. Benzene has a specific gravity of 0.88, a molecular weight of 78, and a vapor density of 2.69. It has a flash point of 12 F, an ignition temperature of 1,044 F, and flammable limits of from 1.3% to 8% (Fire, 1988). Benzene boils at 176 F, freezes at 41.9 F, and is very slightly soluble in water (Hadley & Armstrong, 1991).

Benzene doesn't react with water or with many common chemicals. It will, however, react with all strong oxidizing agents, including chlorine, oxygen, ozone, perchlorates, permanganates, and peroxides.

Many health hazards have been linked to benzene exposure. Although primarily an inhalation hazard, benzene absorption through the skin tissue is also possible. Inhalation of excessive concentration over extended periods of time can effect central nervous system function, while

systemic adsorption may cause depression of the hematopoietic system, aplastic anemia, and leukemia (CFR 29, 1991).

Emission Standards. On March 7, 1990, the Environmental Protection Agency (EPA), published final emission standards for wastes containing benzene under the National Emission Standards for Hazardous Air Pollutants (NESHAP) program established under Section 112 of the CAAA. The action added Subpart FF-National Emission Standard for Benzene Waste Operations to 40 CFR Part 61. Standards set under this regulation state that the benzene control device must achieve a total organic compound concentration of no greater than 20 ppmv (CFR 40, 1991).

Permissible exposure limits (PELS) have been established under 29 CFR Part 1910.1028. These include a time-weighted average limit (TWA) of 1 ppm, and a short-term exposure limit (STEL) of 5 ppm. The Occupational Safety and Health Administration set the TWA limits to ensure that no employee is exposed to an airborne concentration in excess of the imposed limit over an 8-hour time-weighted average. The STEL is based upon airborne concentrations as averaged over any 15 minute period (CFR 29, 1991).

It is estimated that half the U.S. population is exposed to benzene emissions from industrial sources, while virtually the whole population is exposed to benzene emissions from cars . The strict new benzene vapor

emission controls set by the EPA would lead to 99 per cent of the exposed population facing a risk of less than one chance in a million that they develop cancer as a result of benzene emissions.

Benzene - Treatment Options

Conventional Water Treatment. In general, conventional water treatment (coagulation, flocculation, sedimentation, and filtration) is not effective for removal of benzene and most other VOC's from contaminated water sources.

Following spills, VOC's were found to pass through surface water treatment plants with little or no removal accomplished (Seeger et al, 1978). Any losses which are achieved are likely the result of evaporation from open basins.

Oxidation and Ultraviolet Irradiation. The U.S. EPA's Drinking Water Research Division (EPA-DWRD) found no reduction in benzene concentration following treatment with chlorine, chlorine dioxide, or hydrogen peroxide. Using permanganate iron or ferrate iron, no control of benzene or other aromatics were observed (Miltner, 1984). Ultraviolet irradiation was found by the EPA-DWRD to reduce benzene concentrations. There are some commercial processes available which combine ultraviolet irradiation and ozonation; however the mechanisms and end products are not well defined. Reverse osmosis techniques by thin-film

composite membranes is a process control method which has given mixed results. When considering the relatively high cost, other alternatives are usually chosen.

Aeration. Aeration is one of most commonly employed techniques used to control VOC contaminated water supplies. Aeration can be broadly categorized in two ways: (1) putting air through water and, (2) putting water through air. In the air through water systems, mass transfer takes place at the bubble surface and the practice upper limit for the air-to-water ratio is approximately 20 to 1 (volume to volume). The water through air systems create water droplets or a thin layer of water to facilitate mass transfer. Although air-to-water ratios as high as 3000 to 1 have been reported (McCarty, 1983), the air-to-water ratio is generally less than 100 to 1 (EPA-625, 1985). Common air through water aeration devices include; a) diffused-air aeration systems, b) air-lift pumps, and c) mechanical surface aerators. Water through air systems include; a) packed tower aerators, b) tray aeration units, and c) spray and venturi draft aeration devices.

Aeration however, is not a technology that destroys or alters VOC's; it simply transfers them to the ambient air where they are dispersed, diluted and sometimes photochemically degraded. Many states now require "Best Available Technology" (BAT), to be applied to VOC treatment

devices discharging to the air. Most states set emission standards based upon carcinogenic risk. It is common for Allowable Source Impact Levels (ASILs) for carcinogens such as benzene to be set according to an incremental cancer risk level of 10^{-6} . The Safe Drinking Water Act (SDWA) acknowledges that air stripping & granular activated carbon units (GAC) are BAT for treatment of most VOC's. However, in circumstances in which high off-gas concentrations exist, or extremely strict state and local ambient air-quality standards exist, alternative treatment measures may be necessary. These treatment techniques typically consist of a catalytic or thermal incinerator unit.

Regulations enacted under the Resource Conservation and Recovery Act (RCRA) of 1976, as reauthorized in 1985, mandate that incinerators achieve a destruction removal efficiency of 99.99% for all waste materials designated as hazardous. To achieve the required degree of destruction, incinerators operate at temperatures often greater than 1600 C and in highly acidic environments. The generation of such high temperatures requires the use of large amounts of fossil fuel when incinerating low-BTU wastes. The acidic environment, in conjunction with the high temperatures, can result in reduced service life and increased unit maintenance. According to recent projections an estimated 2.5 million tons of contaminated soils (with very low BTU's) await disposal (McGaughy et al, 1984). The resulting fuel and energy costs required for incineration of the associated

off-gas emissions would be extremely high. Thus there is a clear need to develop new, efficient, cost-effective off-gas disposal technologies.

The potential for heterogeneous photocatalytic reactors to fill the void in providing off-gas emission control is still a matter of conjecture. The scope of this research is to examine how one common VOC, benzene, reacts to various conditions which may be encountered during typical off-gas treatment using a TiO_2 photocatalytic fluidized-bed reactor.

Research Goals

The approach of this research was conducted with the intent of matching conditions which may be encountered in field applications of the reactor unit. Specifically, the following questions will be addressed:

1. What effect does influent concentration and flow rate have on overall removal efficiency?
2. What role does humidity, temperature and reaction time have on photocatalytic process kinetics?
3. How much of a factor is adsorption in the overall removal process?

The remainder of this report is divided into the following chapters: Literature Review, Materials and Methods, Experimental Results and Discussion, and Summary & Recommendations.

CHAPTER II

LITERATURE REVIEW

Photocatalytic degradation of organic pollutants in the aqueous phase has been an area of much research (Fujihira et al, 1981; Pruden and Ollis, 1983; Izumi et al, 1980; Kormann et al, 1991). However no previous work could be located in the literature which specifically focused on the photocatalytic reactions of gaseous phase dilute benzene by near ultraviolet illuminated titanium dioxide. Limited studies have been conducted which involve gas phase oxidations of chlorinated organics using ultraviolet irradiated TiO_2 (Dibble and Raupp, 1992) and silica gel and aluminum oxide (Gab et al 1977). This remainder of this literature review is subdivided as follows: photochemical principals, titanium dioxide/semiconductor properties, liquid phase photocatalytic oxidation review, gaseous phase photocatalytic review.

Photochemical Principals

In the natural environment, an organic chemical's ability to absorb sunlight and undergo transformations to new molecular species is generally referred to as photo-transformation or photolysis (Neely & Blau, 1984). Such

photochemical reactions can be classified as processes driven via energy derived from the sun's short wavelength ultraviolet quanta (photons). The potential energy of these ultraviolet photons is comparably higher than the visible and the infrared. Initially a molecule absorbs a photon of light and is raised to an excited state. As the molecule returns to it's original ground state, a number of reactions can take place. Ideally, a molecular bond is broken and the resulting molecule absorbs another photon with the similar end result. A repetitive process occurs until complete degradation to inorganic compounds is achieved. Under ambient temperature regimes, the high energy ultraviolet photon must be present to accomplish this photochemical transformation. Should higher temperatures or higher photo energy concentrations be available, the corresponding degradation potential is increased significantly (Sutton et al, 1985).

In the laboratory, photolysis and other photochemical processes have been researched as possible degradative mechanisms in carcinogenic chemical applications. Artificial sources of ultraviolet radiation in combination with an oxidant or catalyst have been developed and successfully employed in hazardous waste treatment sites. Such systems typically rely on indirect photolysis as their destructive driving mechanism. The kinetics of an indirect photolytic system are based on the interactions of the ultraviolet energy and the oxidant or catalyst. The

resulting chemical reactions may produce a hydroxyl radical which in turn acts as an oxidizing agent and initiates a series of reactions which ultimately destroy the contaminants. These systems contrast direct photolytic reactors in which absorption of photons leads to a break in molecular bonding structure, which in the presence of O₂ or H₂O will cause mineralization - conversion to CO₂ and H₂O (Roy, 1991). Understanding the role of the catalyst in the potentially complex reactions which drive a photocatalytic process is crucial.

Titanium Dioxide-Semiconductor

Properties

Titanium dioxide (TiO₂), is one of the most frequently studied semiconductors. Applications of TiO₂ research can be found in such fields as pigments (Wiseman, 1976), catalysts (Boonstra et al, 1975; and Green, 1980), photocatalysis (Picat et al, 1982; and Izumi et al, 1980) and model oxide systems for surface electrochemical studies. Reported surface phenomena and characteristics are totally dependent upon surface properties, which are undoubtedly quite different from one experiment to the next. Surface properties of TiO₂ are a function of the method of preparation, crystalline structure, surface area, and presence or absence of impurities (Pelizzetti, 1983).

Titanium dioxide exists in three distinct crystalline forms, namely; anatase, rutile, and brookite. The physical

chemical properties of each TiO_2 crystalline structure can be found in the appendix. Titanium dioxide in both the anatase and rutile crystalline forms is colorless and appears white in powdered form. Crystalline titanium dioxide is the most widely used white pigment in commercial applications. This is due mainly to its relatively high refractive index capabilities (Pelizzetti, 1983).

Of the three crystalline forms, anatase seems to be used in most photochemical research applications. Some studies suggest anatase exhibits more electron activity than rutile (Radford et al, 1983). The fact that anatase is converted to rutile at temperatures above 1000 C limits its use in many thermal applications (Dibble, 1989). Brookite is quite rare and no applications could be found involving photocatalytic research.

Titanium dioxide is a metal-oxide semiconductor. Semiconductors differ from most metallic substances in that they do not possess a continuum of electronic energy states. They are however, characterized by an energy gap (band gap) separating the conduction band from the valence band. The valence band (the highest occupied energy state) is constituted by occupied bonding electronic states, while the conduction band (the lowest energy level) contains non-bonding or anti-bonding energy states which are normally unoccupied (Gerischer, 1983). Fermi statistics is used to estimate the distribution potential of electrons amongst the various energy levels. Occupation probability $F(E-E_F)$ can

estimated by the following Fermi equation:

$$F(E-E_F) = (1 + \exp((E-E_F)/kT))^{-1}$$

where: E_F = Fermi energy
E = Electron energy level
k = Boltzman's constant
T = Temperature

From the equation above it is evident that when $E=E_F$ the probability of occupation is equal to fifty percent (Gerischer, 1985).

A semiconductor may exhibit conductivity which can be defined as either n-type (mobile electrons in the conduction band) or p-type (mobile holes in the valence band) (Maruska and Ghosh, 1978). Titanium dioxide is considered to be an n-type semiconductor. N-type semiconductor materials contain electronic donor states in the band gap at levels close to the conduction band. Such a configuration allows for dissociation of an electron into the band gap, thus creating conductivity therein.

Photocatalytic reaction over n-type semiconductors is based upon the following phenomenon. When energy via photon absorbance is equal to or greater than the energy exhibited in the band gap, an electron is excited from the valence band into the conduction band. This results in the creation of a positive hole in the valence band. In the presence of electrophillic species such as O_2 , the surface may be covered by negatively absorbed species, which attract the positively charged photo-produced hole to the surface.

Electrical neutrality is established as the electron holes are essentially scavenged by any oxidizable species present (i.e. H_2O , H_2O_2 , or hydrocarbons) (Pichat, 1982). Research by Formenti et al (1971), showed that when TiO_2 is exposed to energy levels lower than the band gap ($< 3.0 \text{ eV}$), donor impurity levels in the band gap may be excited into the conduction band without formation of positive holes. Although this enables the formation of an $\text{O}^-_{2(\text{ads})}$ species, no interaction between the hydrocarbon (in this case a paraffin) and the oxygen was noted. Thus Formenti concluded that the generation of activated complexes necessary for heterogeneous photocatalytic reactivity are formed only when positive holes are present.

This underlying principal is repeated time and again in the literature. Adsorbed oxygen or hydroxyl species on the titanium dioxide surface will enable the recombination of photo-produced electrons and holes thus providing the necessary mechanisms to drive the heterogenous partial or total oxidations of various organic compounds.

Photocatalytic Research Involving

Liquid Phase Organics

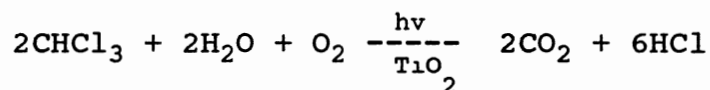
Photocatalytic research of aqueous aromatic solutions is more prevalent than gaseous phase work. Fujihir et al (1981), exposed aromatic compounds including benzene, toluene, and acetophenol to ultraviolet irradiated aqueous suspensions of titanium dioxide. His work concluded that

such compounds could be hydroxylated to the corresponding phenols, biphenyl from benzene, benzaldehyde from toluene, and phenol from acetophenol. Fujihir surmised that H₂O₂ was formed on the titanium dioxide powders as a direct result of photosynthetic reduction of oxygen. The H₂O₂ in direct contact with the semiconductor electrons provided the mechanism for successful heterogeneous photocatalytic oxidation of the aromatics introduced. Fujihir concluded that O₂ and illumination were both required entities of the oxidation process.

Izumi et al (1980) performed successful photocatalytic oxidations of hydrocarbons on platinized titanium dioxide powders. His work demonstrated that photodecomposition of reaction intermediates could be achieved.

Izumi showed phenol, a reaction intermediate in the decomposition of benzene, could be photocatalytically broken down at room temperature into CO₂. Several other aliphatic hydrocarbons, in which alcohols are intermediates, were also successfully photodecomposed.

Work by Pruden and Ollis (1983), examined the degradation of chloroform in illuminated suspensions of titanium dioxide. The following stoichiometry was developed:



Complete mineralization to inorganic compounds was achieved

with quantum efficiencies ranging from 3.3% to 3.9%. Quantum efficiencies are used to relate the molecules of a particular substance converted to the number of photons entering a slurry-free reactor.

Kormann et al (1991) examined the photochemical reaction of chloroform over aqueous titanium dioxide suspensions in greater detail. Their work showed that the adsorption of electron donors and acceptors to the titanium dioxide surface plays a very important role in determining the rate of photocatalytic reactions. Their study likewise surmised that quantum efficiencies for degradation of CHCl_3 is inversely proportional to the square root of the incident light intensity.

Cundall et al (1976) examined the oxidation of several alcohols in the liquid phase via semiconductor dispersions. His work showed that the photocatalytic oxidation of isopropanol to acetone could be achieved with quantum efficiencies approaching 40 percent.

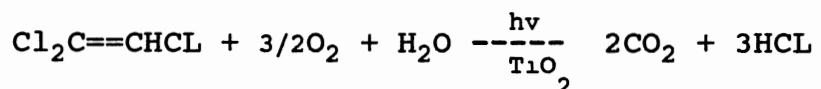
D'Oliveira et al (1990), studied the photocatalytic degradations of two chlorinated aromatic pollutants, 2-chlorophenol (2CP) and 3-chlorophenol (3CP), in titanium dioxide aqueous suspensions at wavelengths of 340 nm. His work studied the effects of illumination, concentration and pH on overall reaction rates. He found that complete mineralization of the pollutants could eventually be achieved, however the time required to attain this state was substantially greater than simple dechlorination and

dearomatization. The most prominent intermediate, via hydroxylation, in the photodegradation of 2 and 3-chlorophenol is chlorohydroquinone. Catechol (CT), was also present, however to a much lesser extent. Further hydroxylation of these intermediates leads to carboxylic acids and unidentified carbonayl compounds. D'Oliveira showed that the decomposition rate was not influenced to any great extent by changes in pH over a wide range. Further, the heterogeneous photocatalysis did not require any chemical aside from oxygen in the form of air, to complete the reactions. Optimal quantum efficiencies were found to increase with increasing radiant flux. Initial rates of photocatalytic transformations of 3CP were shown to increase sharply and then steadily level off with increasing initial concentrations. At very low concentrations of pollutant, the efficiency of the degradation decreased. D'Oliveira concluded that since the reaction was essentially a surface phenomena, competition for surface sites at low concentrations tend to lead to lower degradation rates. This theory is further explored and readily substantiated by researchers working on photocatalytic reactions in the gaseous phase.

Photocatalytic Research Involving Gaseous Phase Organics.

Dibble and Raupp (1992), provide a comprehensive study involving gas-solid heterogeneous photocatalytic reactions.

In their work, trichloroethylene (TCE), is successfully oxidized at ambient temperatures via a flat plate fluidized bed photoreactor system. Silica-supported titanium dioxide is used as the catalyst, which is exposed to near ultraviolet irradiation and gaseous TCE. The TCE was oxidized via the following stoichiometric reaction:



Their experiments studied the effects flow rate, TCE concentration and water vapor concentration had on reactor performance.

Reactor performance was evaluated based on TCE conversion and global reaction rates. The global reaction rate (R_g) was defined as the overall rate at which TCE is oxidized per unit mass of reactor bed ($\mu\text{mol g}^{-1} \text{min}^{-1}$). Dibble found that a decrease in total influent feed rate while holding TCE concentration constant, increases TCE conversion. Global reaction rates remained relatively unchanged under this scenario. This, Dibble explains, reflects the first order nature of the reaction with respect to TCE concentration and the plug flow nature of the gas through the bed.

At low concentrations (5.5 ppm) TCE conversion approaches 100 percent; however the global reaction rate is substantially decreased. Thus TCE feed rate is found to be the controlling factor on observed reaction rates under high

conversion scenarios.

Dibble's work also showed that fluctuation in relative humidity did not affect oxidation rates at relatively low concentrations of TCE influent feed. However, at higher concentrations, the rate of oxidation is vastly influenced by water vapor concentration. Dibble also reported that catalytic activity in the absence of ultraviolet illumination could be sustained for a brief period of time. Dibble noted that activation times of approximately one hour upon initial startup of a fresh catalyst bed were required in order to attain maximum photocatalytic activity levels. Quantum efficiencies were reported to be on the order of 2 to 13 percent, which is consistent with similar reported efficiencies of liquid phase photoreactions involving TCE.

Formenti et al (1971) provided some of the earliest work on heterogeneous photocatalytic reactions in the gaseous phase. They reported the partial oxidation of certain paraffins could be sustained via heterogeneous catalytic reactions performed in a differential dynamic fixed-bed reactor. With titanium dioxide as the catalyst, Formenti performed various experiments which studied the catalytic activity as a function of wavelength and temperature. The research found that in the range of 30 to 110 C, photocatalytic activity is not modified to any great extent. At temperatures above 200 C, photocatalytic activity ceases and is replaced by homogeneous free radical reactions (thermal catalytic reactions). At temperatures

below 300 C oxidation of paraffins via thermal catalytic processes over titanium dioxide was unsuccessful; however at temperatures above 300 C the oxidations were complete.

Formenti reported a noticeable change in the color of the catalyst during reaction in the vicinity of 110 C. The catalyst takes on a brownish color which is more pronounced over time. As this color change is occurring, catalytic activity is adversely affected. The white color of the catalyst could be restored at temperatures of 350 C in the presence of oxygen, with a return to photocatalytic activity in the temperature range of 30 to 110 C observed.

Gab et al (1977) conducted research on gas phase oxidations of various chlorinated alkenes, freons, and aromatic hydrocarbons including benzene. In this work, the organics were adsorbed onto silica gel and irradiated with ultraviolet light equivalent to 290 nm. Conversion products of carbon dioxide, chlorine gas and hydrogen chloride were reported. Gab's research showed that aromatic compounds exhibited a much higher persistence with respect to photomineralization in comparison to the chlorinated alkenes and freons. Oxidations of the compounds to the reported conversion products were the likely result of homogeneous reactions rather than heterogeneous photocatalytic reactions based on the fact that silica gel does not absorb in the near ultraviolet (Dibble, 1989).

The oxidation of gaseous alkyltoluenes, $RC_6H_4CH_3$, ($R=C_2H_5$, $(CH_3)_2CH$ and $(CH_3)_3C$) was reported by Mozzanegra et

al (1977), via differential flow photoreactor employing an ultraviolet illuminated fixed bed of titanium dioxide. The work similarly concludes that the aromatic ring is quite resistant to oxidation. It also notes that O₂ to hydrocarbon ratios were highly influential on conversion rates. A low ratio (increased surface coverage of hydrocarbons) tends to limit reported conversion rates.

CHAPTER III

METHODS AND MATERIALS

Experimental Apparatus

The laboratory scale apparatus, as illustrated in Figure 1, was used for all experimental procedures performed for this research. Benzene (69.1 ppm, balance air, from Liquid Air Corp.) and breathing quality air (Sooner Air Gas) were contained in compressed gas cylinders. Two-stage pressure regulators were used to deliver the gaseous reactants to the associated influent lines. All lines were constructed of 1/4 inch or 1/8 inch stainless steel tubing. Water vapor was introduced into the system via a bubbling air saturator system which consisted of a series of three 1000 ml beakers. Two were filled with water and the third was left empty. A digital humidity and temperature probe (U.E.I. Corp. model DTH-1, distributed by Davis Instruments Corp.), was contained and sealed in sampling vessel #1. The probe has an LCD display, and is accurate from ranges of 20 to 90 percent relative humidity and 30 to 200 degrees F. Sampling vessel #1 consists of a 1 1/4 inch diameter cylindrical glass tube five inches in length. The vessel contains a raised 1/4 inch diameter sampling port. The

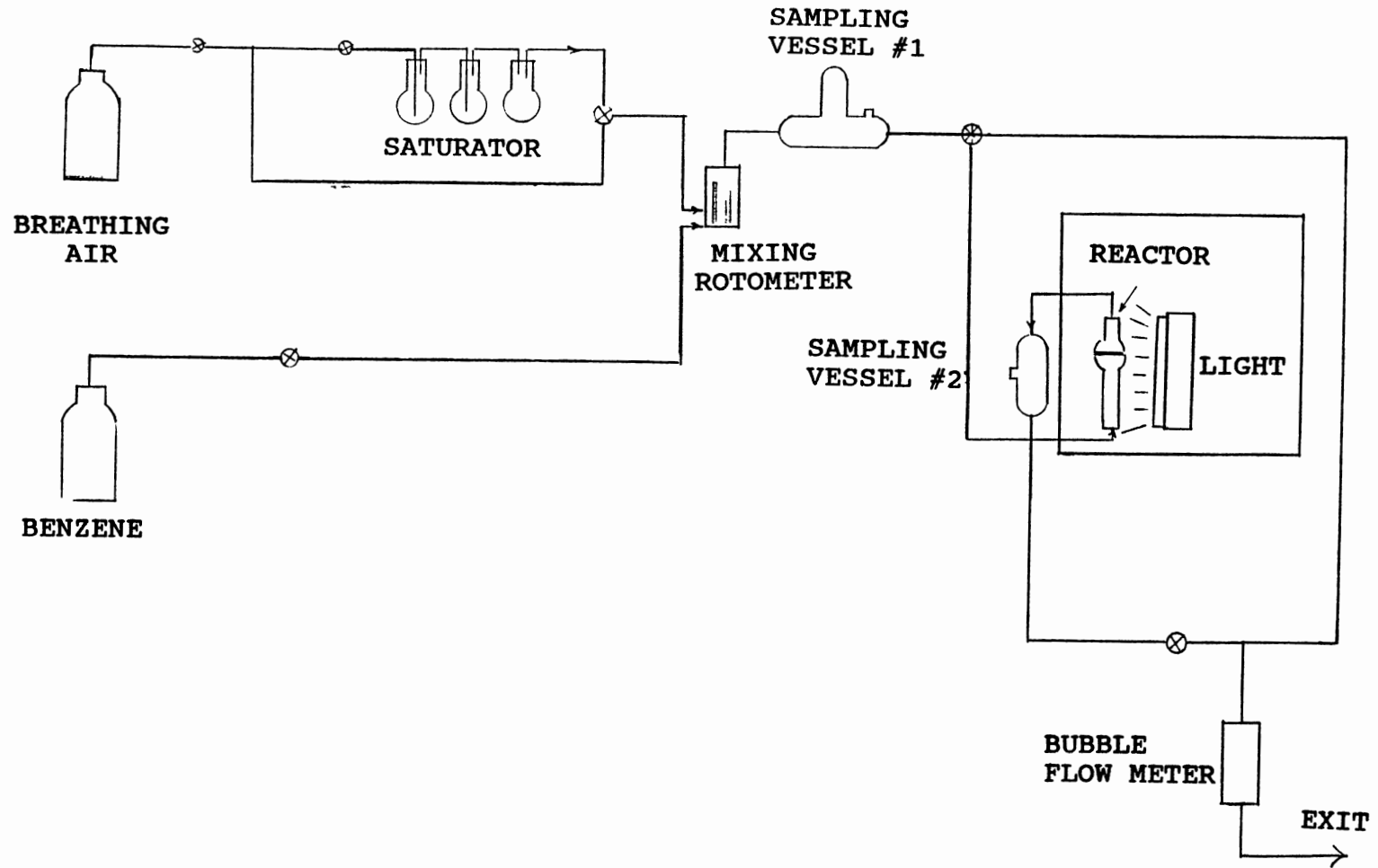


Figure 1. Experimental Apparatus

the volumetric flowrates of the benzene and the air streams is controlled via separate in-line needle valves located directly upstream of the mixing rotameter. Influent benzene and air streams enter the mixing rotameter in separate lines and exit via a single 1/4 inch tubing section. A dual flow rotameter system allows both influent lines to be measured prior to mixing. The rotameter was calibrated prior to initial experimentation. The flow range capability of the meter is 10 - 700 cc/min.

Sampling vessel #2 is a 2 1/2 inch long by 1 inch diameter cylindrical glass tube which has a 1/4 inch raised sampling port. The saturator by-pass line was incorporated in the apparatus during experimental runs which necessitate low relative humidities. The line was not attached during experiments in which the saturator was employed.

All tubing to tubing-and-tubing to fitting connections were Swagelok. All glass-to-tubing connections consisted of a Tygon tubing adaptor seal. This is achieved by fitting a piece of Tygon tubing over the glass and tubing ends and affixing a small hose clamp over the connection to assure an airtight seal. Teflon tape is wrapped around the Tygon prior to clamping down to aid to the integrity of the seal. The bubble flow meter at the downstream end of the apparatus is incorporated into the system via a similar Tygon connection process.

Fluidized-Bed Reactor

An illustration of the fluidized bed reactor is shown in Figure 2. The reactor is designed to allow low pressure drop and high through-put of the influent gases. The reactor is made of flat walled 7042 Pyrex Glass. The upper portion of the reactor is enlarged so as to insure a means of momentum reduction for the fluidized catalyst particles. The overall height of the reactor is 216 mm. It is 33 mm wide (OD) at its largest cross sectional area in the upper portion. The internal reactor diameter is 10.2 mm wide by 2 mm thick in the flat-parallel plate lower section. The reactor is opened via a metal pinch clamp / o-ring joint assembly. An air tight seal is likewise maintained by this assembly. Coarse glass frits are seated in the influent and effluent ends of the reactor. These provide effective containment of the catalyst material while allowing efficient distribution of reactant gas flows.

The reactor is contained in the reactor compartment which consists of a 21" wide x 23" long x 21" high, light restrictive styrofoam box. Exposure to the ultraviolet light source is initiated within the reactor compartment. A 4-watt fluorescent bulb (GE FT5-BLB) is affixed to the back of the compartment so as to allow a parallel orientation at a distance of 0.5 inches from the reactor body.

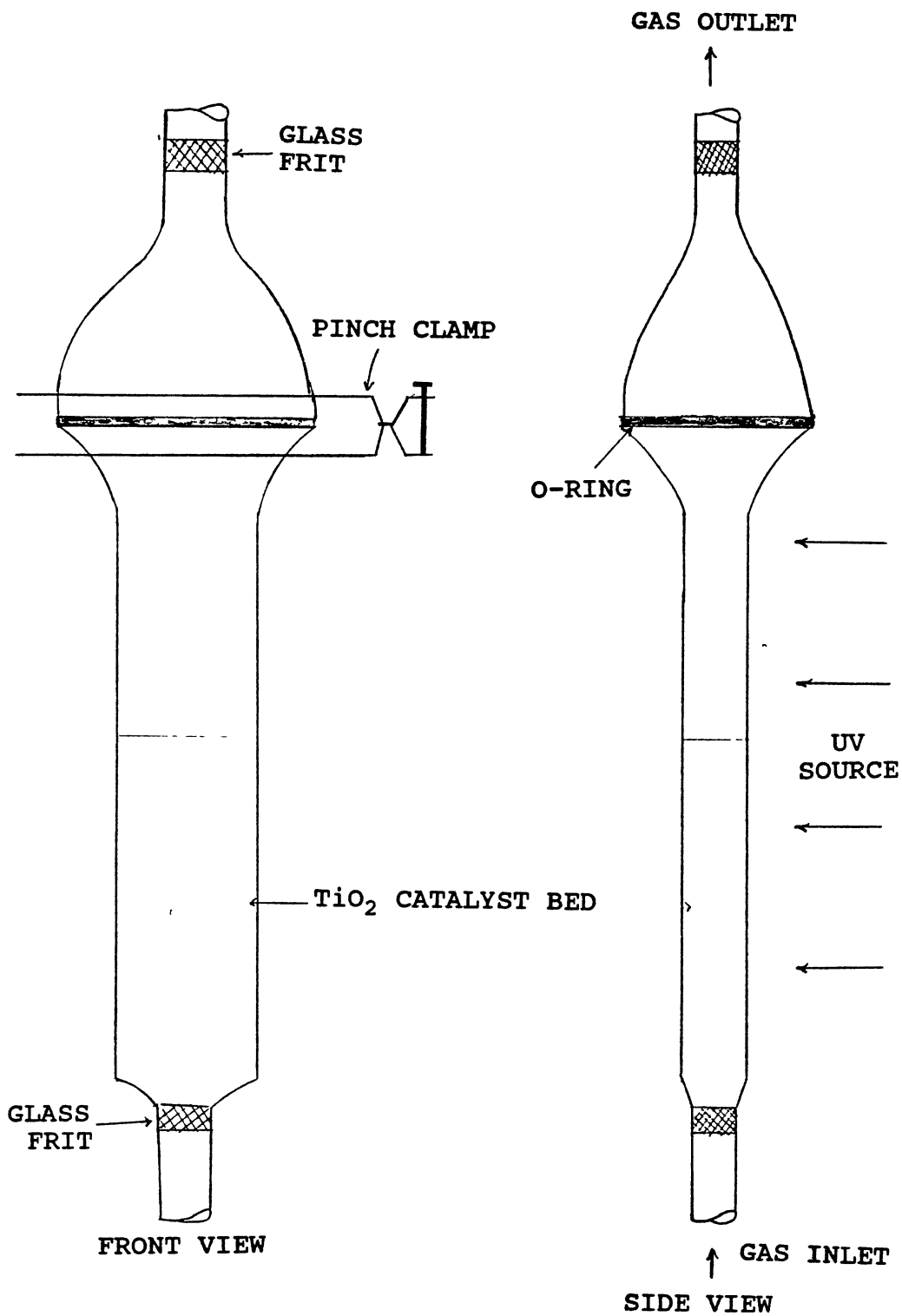


Figure 2. Fluidized-Bed Reactor

Catalyst Preparation

The catalyst used in this research consisted of anatase titanium dioxide crystals which were supported on Davisil 646 silica gel (Aldrich Chemical Co.). This catalyst bed type was chosen due to its published ability to provide adequate fluidization characteristics and efficient reactant-catalyst contact surface area (Dibble, 1989). The method used to load the titanium onto the silica gel is described by Duonghong et al (1981). This method allows colloids of TiO_2 to be impregnated on the silica surface via a low pH solution. The procedure followed to prepare the catalyst is summarized below.

20 ml of Titanium tetraisopropoxide (Aldrich Chemical Co.) is dissolved in 20 ml of 2-propanol (Fisher Chemical Co reagent grade). In a separate beaker, 42 ml of distilled water is acidified to a pH of 1.5 with reagent grade HCL. The 40 ml titanium tetraisopropoxide solution is then slowly added to the acidified water beaker. The resultant slurry consisted of white colloids approximately 1/8 inch in diameter. A 4 gram sample of silica gel is then added to the solution and stirred vigorously for approximately 30 seconds. The resulting TiO_2 / silica gel solution has a pH of 2.7. TiO_2 colloids are stable at a $\text{pH} \leq 3$. The beaker is then sealed and left to evaporate. After a period of four days the isopropanol solution was completely evaporated

and the titanium / silica gel catalyst appeared bright white in color and was granular to powdery in texture. The prepared catalyst was then weighed to determine titanium content. The results of the catalyst preparation are listed in Table II.

TABLE II
CATALYST BED PROPERTIES

| Davisil Gel (gm) | TiO ₂ (gm) | <u>gm TiO₂</u> gm Davisil | <u>gm TiO₂</u> gm catalyst |
|---------------------|--------------------------|---|--|
| 4.000 | 13.079 | 3.269 | 0.766 |

Experimental Techniques

All experiments performed in this research basically followed the same laboratory procedure. The experiments began by turning on the gas chromatograph which necessitated the initialization of the data station collection machine. The fluidized bed reactor is then loaded with a predetermined amount of catalyst in experiments in which a "fresh bed" is required. For this thesis, the catalyst bed weight was held constant at 0.5480 grams in every experiment. This amount resulted in a static bed height of 1.40 inches inside the reactor cavity. After loading the catalyst, the reactor is sealed by firmly closing the adjustable metal clamp.

The benzene and the air flows are then turned on and directed to the exit by-pass line while flow calibrations are set. The ratio of air to benzene is adjusted at the calibrated rotameter and is set to meet experimental parameters desired. The relative humidity and temperature probe located in sample vessel #1 is used to monitor the mixed reactant influent stream. The relative humidity of the gaseous stream is adjusted by regulating the amount of air flowing through the saturator. In experiments where the desired relative humidity is $\leq 23\%$, the saturator may be bypassed totally allowing the air stream to flow directly from the compressed gas cylinder to the mixing chamber.

Samples of the mixed reactant stream are taken from sampling vessel #1 and injected into the G.C. for analysis. Samples are continuously taken until steady benzene peaks matching the desired experimental parameters are consistently recorded by the G.C. At this point the flow is switched from the reactor by-pass line to the reactor influent line via the three-way valve located directly upstream from the reactor. This transition to reactor feed is done gradually so as to assure even fluidization of the catalyst bed. The catalyst bed height under fluidized conditions will range from 2 - 4 inches depending on the flow of the influent gases. The flowrate through the reactor is measured by the bubble flow meter located downstream of sample vessel #2.

Once flowrate is determined, the reactor is ready to be irradiated by the ultraviolet source. Immediately after turning the ultraviolet light on, the experimental time clock is started. Samples from the effluent reactor line are taken from sample vessel #2 and injected into the gas chromatograph for post-reactor analysis. Aside from effluent reactor concentration, the following data is recorded at the time each sample is drawn: sample time, relative humidity, influent temperature, volumetric flowrate, and reactor surface temperature.

CHAPTER IV

RESULTS AND DISCUSSION

A total of twenty-nine experiments were performed under a variety of reactor conditions. The objective of the research was to assess overall reactor performance based on conditions which might be imposed under field applications. With this in mind, the reactor was subjected to a wide range of influent concentrations, volumetric flowrates, and relative humidity scenarios.

Table III summarizes the experimental operative parameters in the order in which the experiments were performed. The steady-state reaction rates and overall benzene removal efficiencies are listed in Table IV. The steady-state reaction rate (or global reaction rate- R_g) is calculated based on the overall rate at which benzene is removed per unit mass of reactor bed ($\mu\text{mole/gm-min}$).

Figures 4.1 to 4.15 represent plots of percent benzene removal achieved vs. time, for each of the experimental runs. Experimental conditions are described on each plot. In the majority of the experiments, flow rates were continuously monitored and are also over played on the accompanying graphs.

TABLE III
EXPERIMENTAL OPERATING PARAMETERS

| Exp. No. | Benzene Conc. (ppm) | Q_R (cm ³ /min) | Rel. Humidity (%) | Figure (#) |
|----------|---------------------|------------------------------|-------------------|------------|
| 1 | 69.1 | 285 | 23.0 | 4.1 |
| 2 | 69.1 | 283 | 23.0 | 4.2 |
| 3 | 69.1 | 240 | 24.5 | 4.3 |
| 4 | 34.7 | 201 | 40.0 | 4.4 |
| 5 | 33.9 | 249 | 23.0 | 4.5 |
| 6 | 69.1 | 336 | 21.0 | 4.6 |
| 6A | 49.4 | 218 | 46.0 | 4.6 |
| 7 | 69.1 | 328 | 22.0 | 4.7 |
| 7A | 69.1 | 196 | 22.0 | 4.7 |
| 7B | 69.1 | 114 | 22.0 | 4.7 |
| 7C | 44.0 | 349 | 22.0 | 4.7 |
| 8 | 34.9 | 300 | 22.0 | 4.8 |
| 8A | 32.8 | 134 | 22.0 | 4.8 |
| 8B | 33.2 | 240 | 22.0 | 4.8 |
| 8C | 33.6 | 262 | 22.0 | 4.8 |
| 9 | 21.1 | 334 | 22.0 | 4.9 |
| 9A | 20.0 | 252 | 22.0 | 4.9 |
| 9B | 22.0 | 392 | 22.0 | 4.9 |
| 10 | 6.4 | 320 | 22.5 | 4.10 |
| 10A | 8.0 | 236 | 22.3 | 4.10 |
| 11 | 10.4 | 338 | 60.0 | 4.11 |
| 12 | 8.4 | 280 | 39.8 | 4.12 |
| 12A | 10.5 | 346 | 30.8 | 4.12 |
| 13 | 35.9 | 361 | 21.5 | 4.13 |
| 14 | 21.6 | 320 | 60.0 | 4.14 |
| 15 | 7.2 | 233 | 23.5 | 4.15 |
| 15A | 6.4 | 155 | 21.0 | 4.15 |
| 16 | 8.1 | 315 | 24.0 | 4.16 |
| 17 | 7.6 | 302 | 25.0 | 4.17 |

TABLE IV
EXPERIMENTAL REACTION RATES

| Exp. No. | $R_g(\frac{\text{umole C}_6\text{H}_6}{\text{gm cat-min}})$ | C_6H_6 Removal Efficiency (%) | $R_g(\frac{\text{umole C}_6\text{H}_6}{\text{gm TiO}_2\text{-min}})$ |
|----------|---|---|--|
| 1 | 0.753 | 51.4 | 0.983 |
| 2 | 0.313 | 21.5 | 0.408 |
| 3 | 0.563 | 45.6 | 0.735 |
| 4 | 0.035 | 6.7 | 0.045 |
| 5 | 0.059 | 9.4 | 0.077 |
| 6 | 0.885 | 51.2 | 1.155 |
| 6A | 0.060 | 7.5 | 0.078 |
| 7 | 0.747 | 44.3 | 0.975 |
| 7A | 0.283 | 28.1 | 0.369 |
| 7B | 0.132 | 22.6 | 0.172 |
| 7C | 0.092 | 8.0 | 0.120 |
| 8 | 0.086 | 11.1 | 0.112 |
| 8A | 0.002 | 0.5 | 0.002 |
| 8B | 0.025 | 4.2 | 0.032 |
| 8C | 0.058 | 8.9 | 0.075 |
| 9 | 0.278 | 53.1 | 0.363 |
| 9A | 0.126 | 33.7 | 0.164 |
| 9B | 0.239 | 37.2 | 0.317 |
| 10 | 0.152 | 100.0 | 0.198 |
| 10A | 0.141 | 100.0 | 0.184 |
| 11 | 0.054 | 20.9 | 0.070 |
| 12 | 0.023 | 13.6 | 0.030 |
| 12A | 0.052 | 19.2 | 0.067 |
| 13 | 0.402 | 41.7 | 0.525 |
| 14 | 0.059 | 11.5 | 0.077 |
| 15 | 0.125 | 100.0 | 0.163 |
| 15A | 0.073 | 100.0 | 0.095 |
| 16 | 0.190 | 100.0 | 0.248 |
| 17 | 0.170 | 100.0 | 0.222 |

Results

A review of the experimental data presented in Figures 3 - 17 provide evidence of a few interesting reaction characteristics. The first which will be examined is photocatalytic activation rates. In every experiment in which a fresh catalyst bed is used, an initial conditioning time of between 40 to 90 minutes is necessary in order to reach optimal levels of photocatalytic activity in the reactor (please refer to Fig. 3. for an appropriate example). Table V lists the activation times recorded for each "fresh-bed" experiment. The average time for the thirteen experimental runs listed is approximately 60 minutes.

Removal efficiencies of 44 to 51 percent were consistently achieved during low humidity (22% - 24%), high concentration runs (69.1 ppm). Please refer to Figures 3., 5., 8., & 9. Steady-state global reaction rates for these runs ranged from 0.56 to 0.88 umole of benzene (g of catalyst)⁻¹ min⁻¹, or between 0.7 to 1.2 umole benzene (g of TiO₂)⁻¹ min⁻¹.

Experiments in which dilute levels of benzene were tested (6 to 10 ppm), removal efficiencies of up to 100% were established under a variety of flow regimes. Once attained, these conversion rates were sustained for the extent of the experiment and seemed unresponsive to fluctuations in volumetric flowrate (please refer to figs 11. and 17.).

TABLE V
PHOTOCATALYTIC ACTIVATION RATES

| Exp. No. | Photocatalytic Activation* (minutes) |
|-------------|---|
| 1 | 69 |
| 3 | 84 |
| 4 | 40 |
| 6 | 56 |
| 7 | 45 |
| 8 | 41 |
| 9 | 40 |
| 10 | 39 |
| 11 | 44 |
| 12 | 86 |
| 13 | 56 |
| 14 | 84 |
| 15 | 87 |

* photocatalytic activation represents the on-stream time required for a fresh catalyst bed to reach maximum photocatalytic activity level.

Experiment #2, (Figure 4.) was conducted 24 hours after experiment #1. The experimental conditions were similar. However the catalyst bed was reused in experiment #2. It can be noted that a steady-state reaction is established in less than 15 minutes in experiment #2, which compares to 69 minutes in experiment #1. However, overall removal efficiencies for experiment #2 were 60 percent less than those attained in experiment #1.

Another observed phenomena deals with the physical characteristic of the catalyst. In all experiments in which a steady-state reaction resulted in removal efficiency of 30% or more, the titanium dioxide catalyst changed colors from a pure white to a tannish color. This color change occurred at or near the time the maximum reactor photocatalytic activity was observed.

It can be noted that changes in reactant inlet concentration and humidity severely hamper reactor efficiencies and reaction rates immediately upon implementation of the changes. Good examples of this can be seen in Experiments #5 & #5A , and #6 - #6C. In most cases, photocatalytic activity slowly rebounds, however only to a fraction of the reaction rates prior to these conditional changes in concentration and humidity. Changes in flow were less severe in effects on reactor performance, however their influence is quite discernable. Please refer to Figure 15., Experiment #13. Conversion efficiencies gradually decline in most experiments as flow is reduced.

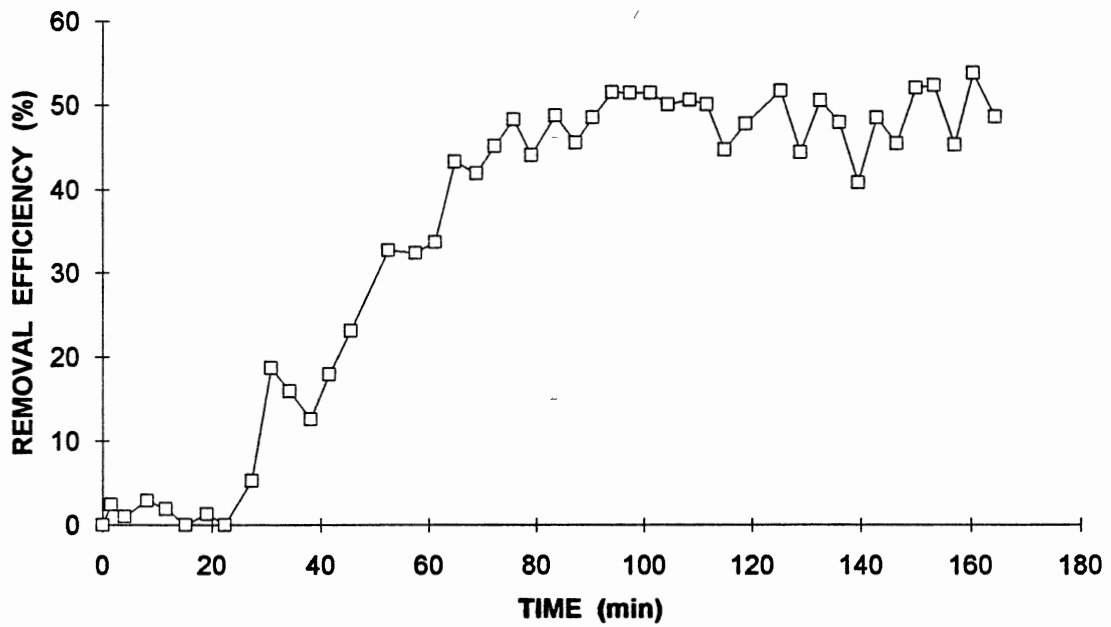


Figure 3. Results of Experiment 1: Conc.= 69.1 ppm C₆H₆, Q_R= 285 cm³/min, Relative Humidity= 23%.

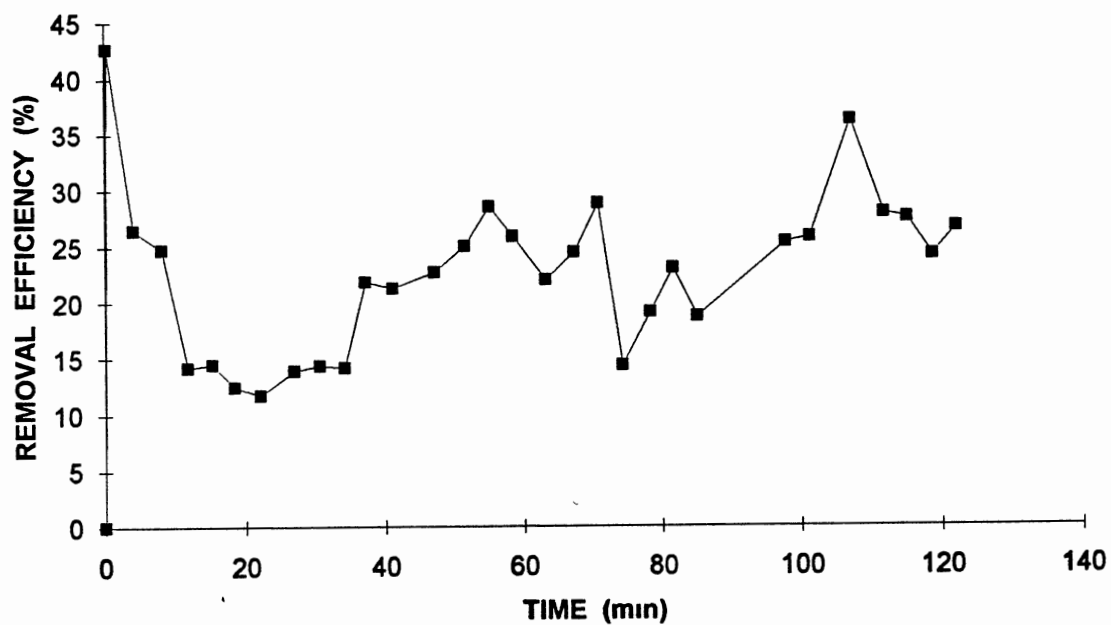


Figure 4. Results of Experiment 2: Catalyst Bed Reused from Exp. 1. Conc.= 69.1 ppm C₆H₆, Q_R= 285 cm³/min
Relative Humidity = 23%.

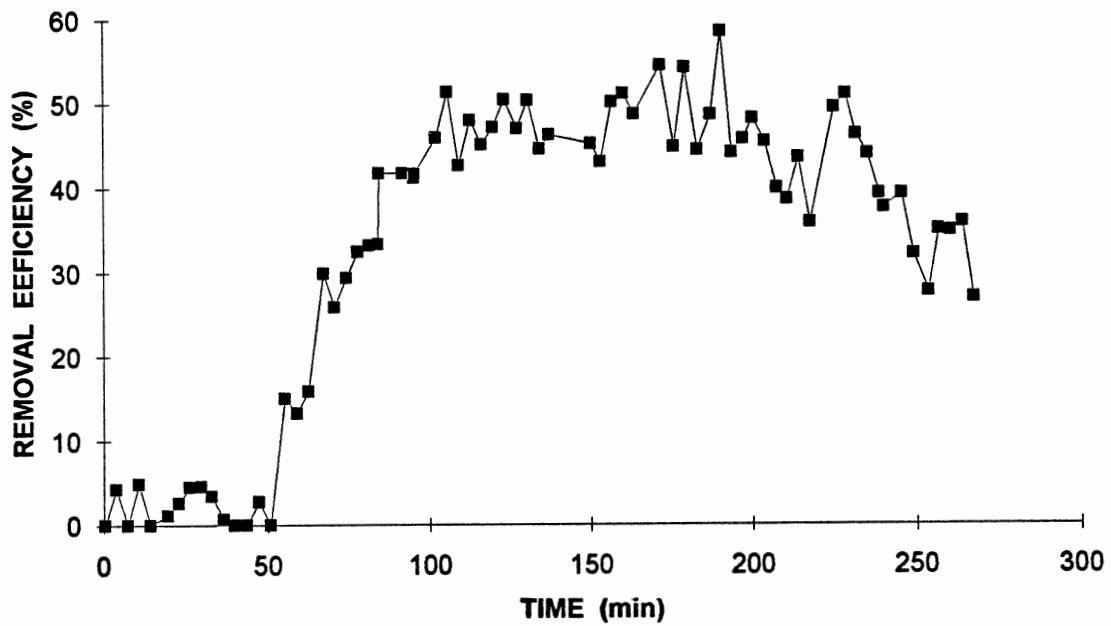


Figure 5. Results of Experiment 3: Conc= 69.1 ppm C₆H₆,
 Q_R= 240 cm³/min, Relative Humidity= 24.5%.

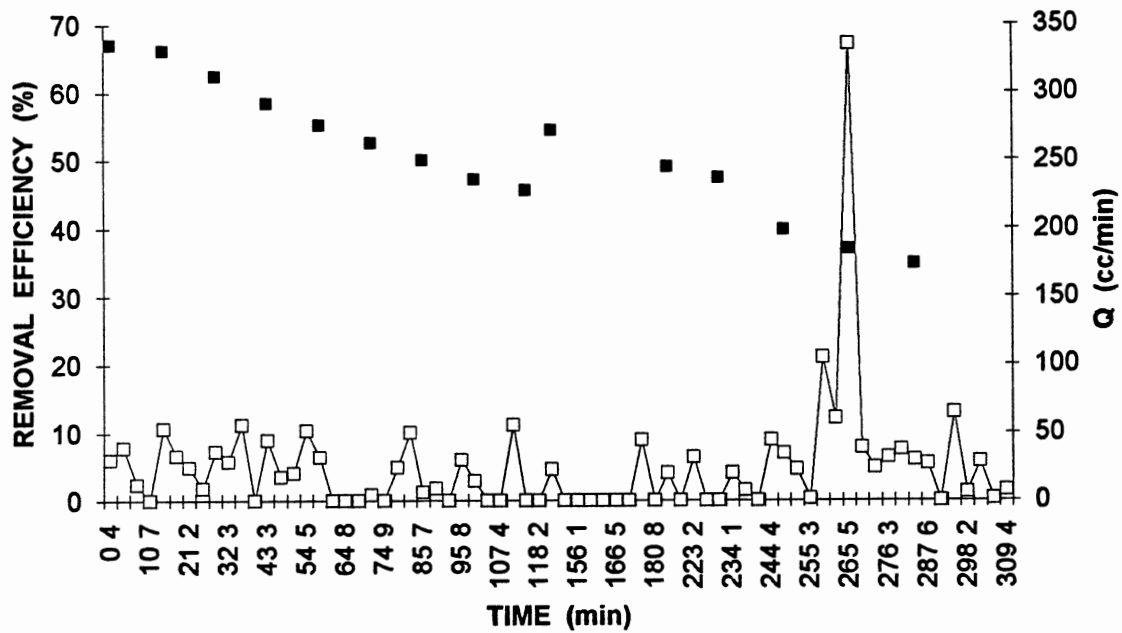


Figure 6. Results of Experiment 4: Conc. = 34.7 ppm C_6H_6 , Relative Humidity = 40%, Initial $Q_R = 335 \text{ cm}^3/\text{min}$.

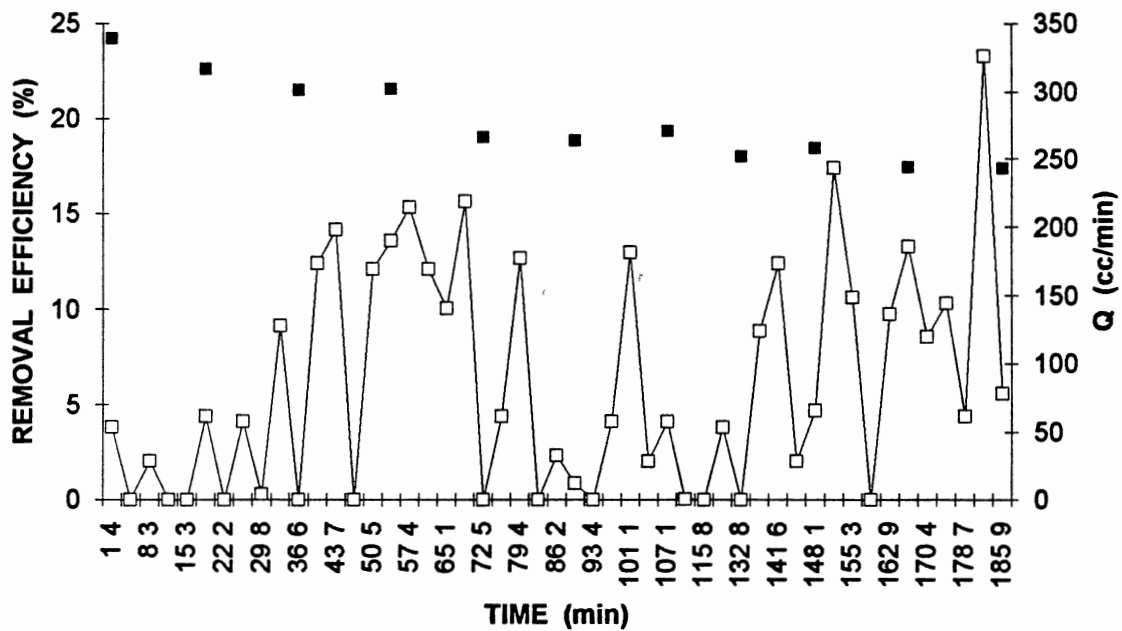


Figure 7. Results of Experiment 5: Conc = 33.9 ppm C₆H₆, Relative Humidity = 23%, Initial Q_R = 339 cm³/min.

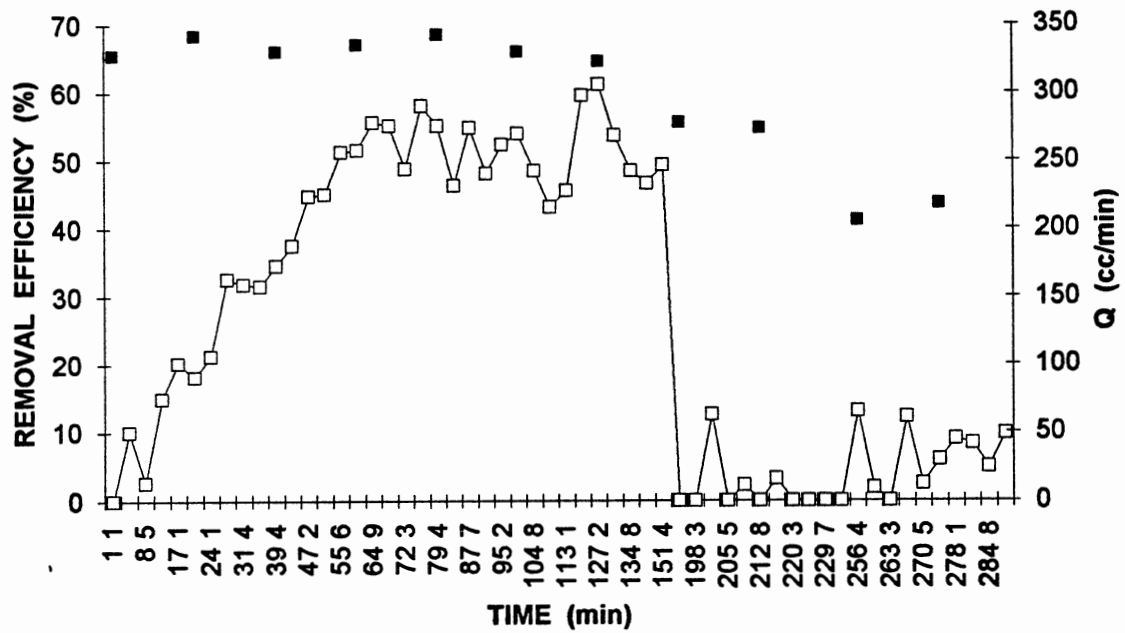


Figure 8. Results of Experiments 6 & 6A. Exp 6: Conc= 69.1 ppm C_6H_6 , Relative Humidity = 21%; Exp 6A: @ 194 min. change Conc. C_6H_6 to 49.4 ppm & Relative Humidity to 46%.

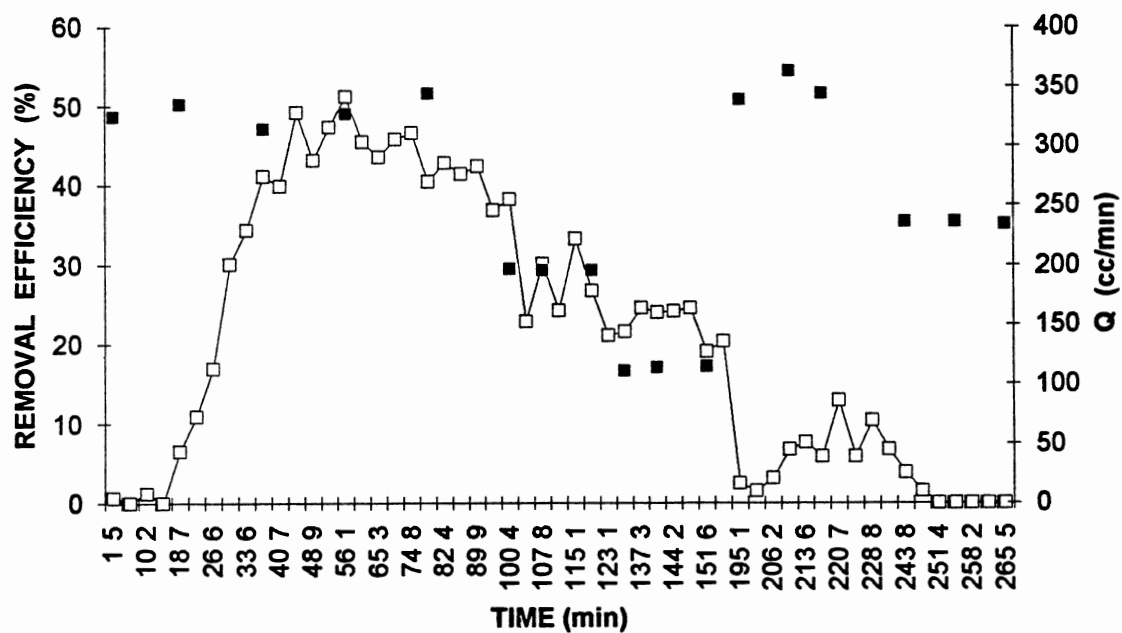


Figure 9. Results of Experiments 7, 7A, 7B, & 7C. Exps. 7, 7A & 7B: Conc. = 69.1 ppm C_6H_6 . Exp. 7A = Q_R change @ 100 minutes. Exp. 7B = Q_R change @ 134 min. Exp. 7C = Conc. change to 44.0 ppm C_6H_6 . Relative Humidity = 22.0% for all experiments.

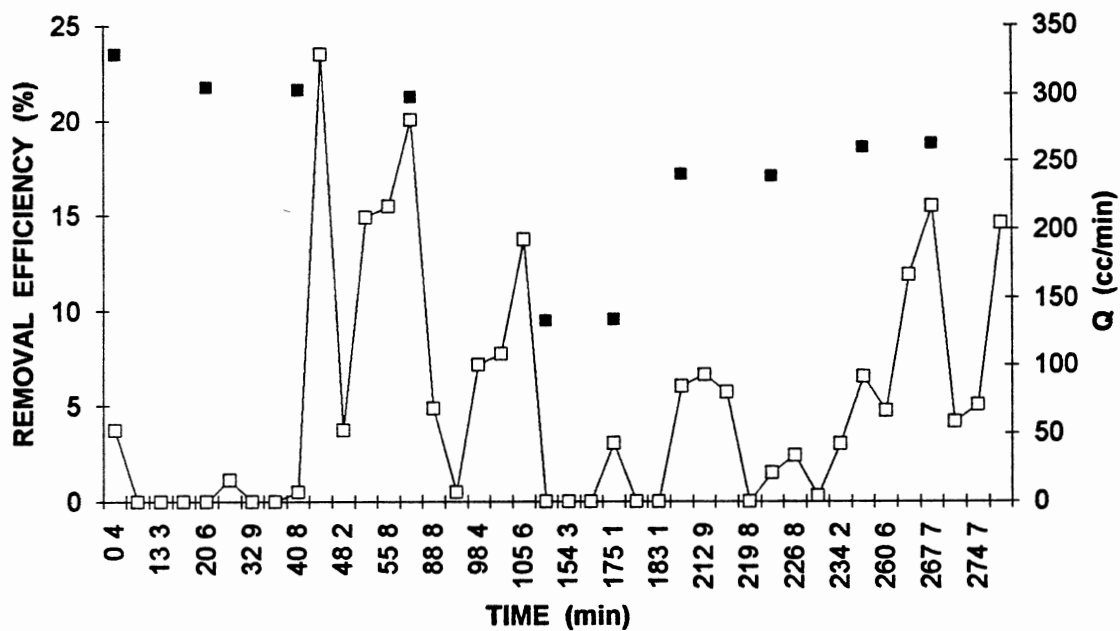


Figure 10. Results of Experiments 8, 8A, 8B & 8C. Exp. 8: Conc. = 34.9 ppm C_6H_6 . Exp. 8A: @ 150 min. Q_R change & Conc. = 32.8 ppm. Exp. 8B: @ 209 min. Q_R change & Conc. = 33.2 ppm. Exp. 8C: @ 257 min. Q_R change & Conc. = 33.6 ppm. Relative Humidity = 22.0% for all experiments.

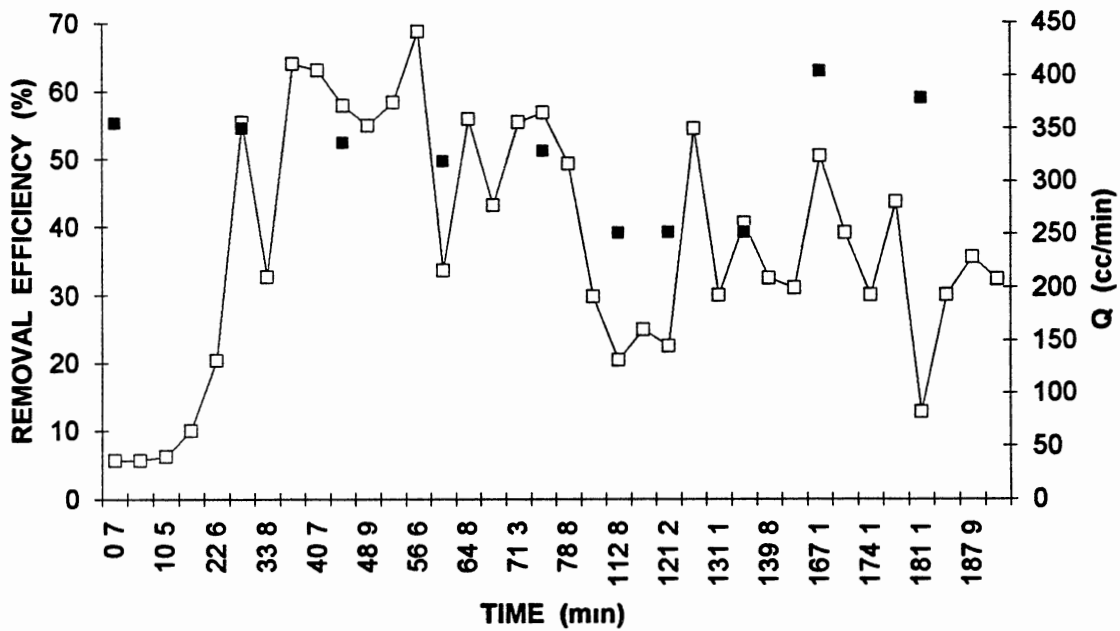


Figure 11. Results of Experiments 9, 9A, & 9B. Exp. 9: Conc. = 21.1 ppm C_6H_6 . Exp. 9A: @ 112 min. Q_R change & Conc. = 20.0 ppm. Exp. 9B: @ 167 min. Q_R change & Conc. = 22.0 ppm. Humidity = 22.0% for all experiments.

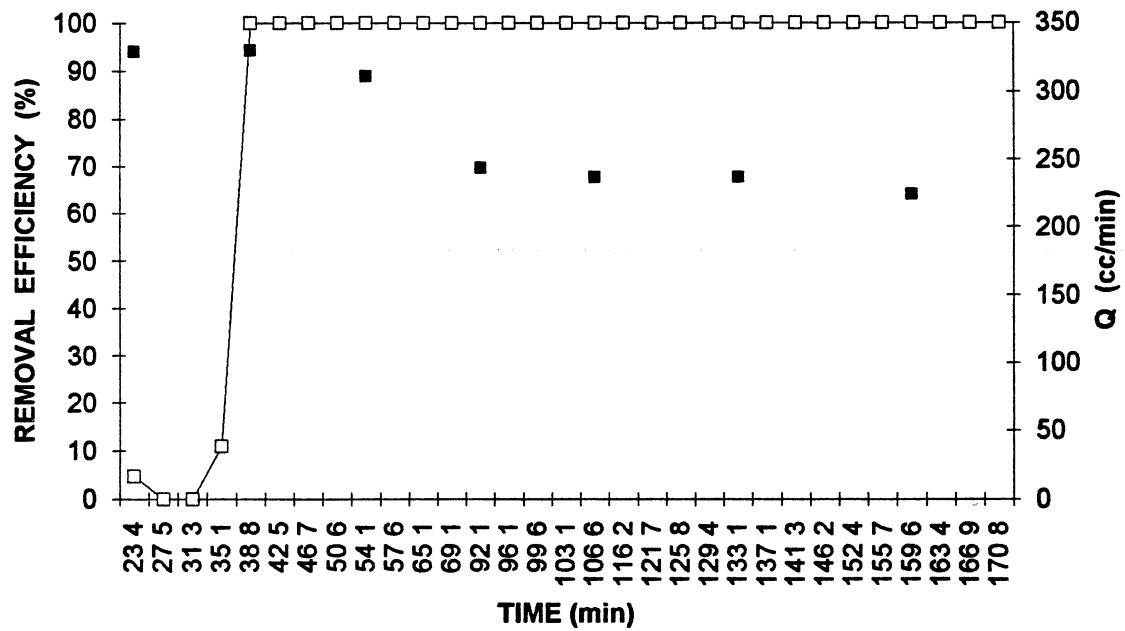


Figure 12. Results of Experiments 10 & 10A. Exp. 10: Conc. = 6.4 ppm C₆H₆. Exp. 10A: @ 92 min. Q_R change & Conc. = 8.0 ppm. Humidity = 22.5 % for both experiments.

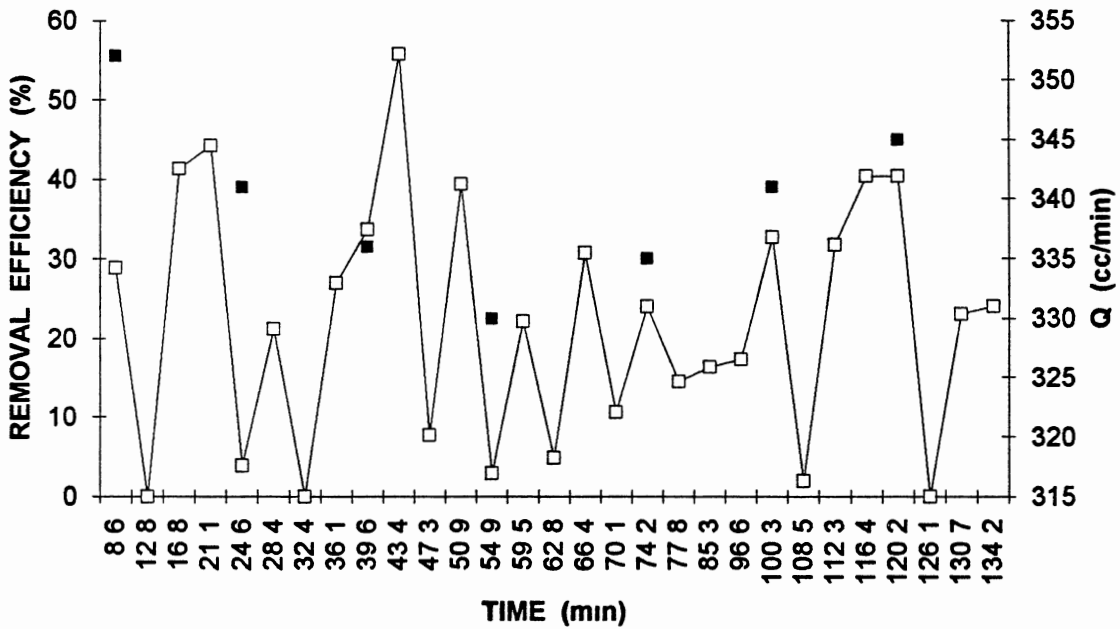


Figure 13. Results of Experiment 11. Conc. = 10.4 ppm C₆H₆, Relative Humidity = 60.0%.

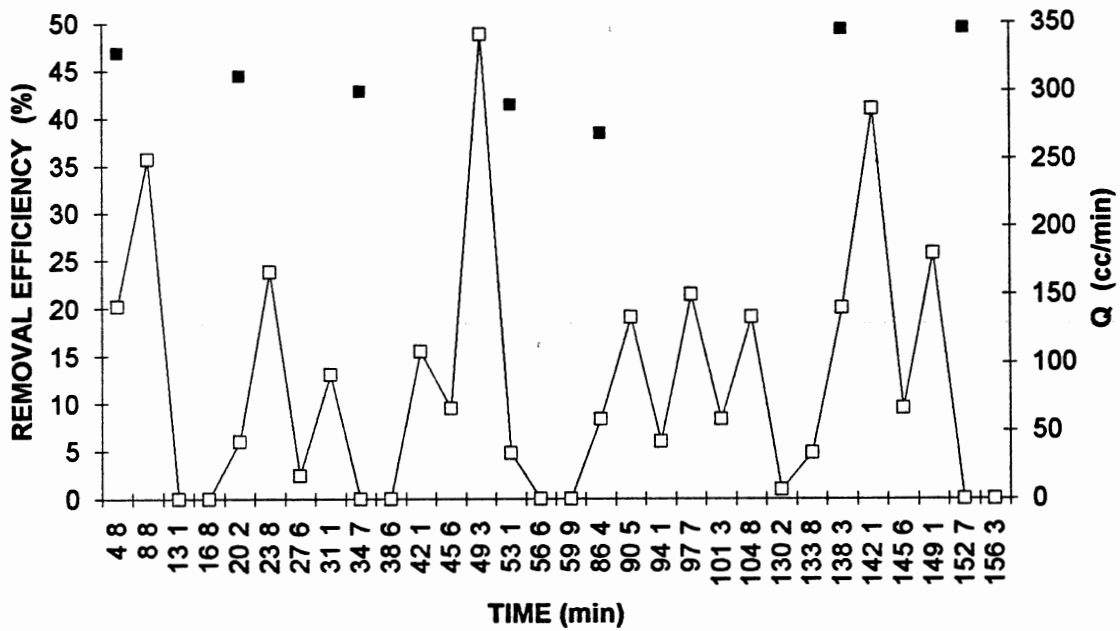


Figure 14. Results of Experiments 12 & 12A. Exp. 12:
 Conc.= 8.4 ppm C₆H₆, Relative Humidity= 39.8%. Exp. 12A:
 @ 130 min. Q_R change & Conc.= 10.5 ppm, Humidity = 30.8%.

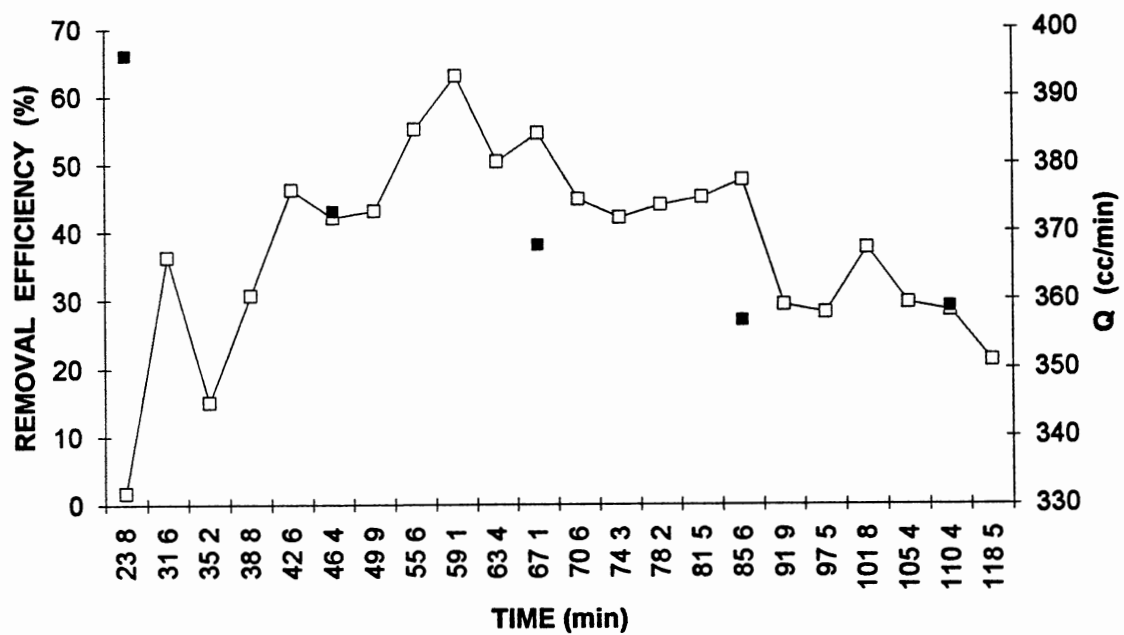


Figure 15. Results of Experiment 13. Conc. = 35.9 ppm C_6H_6 , Relative Humidity = 21.5%.

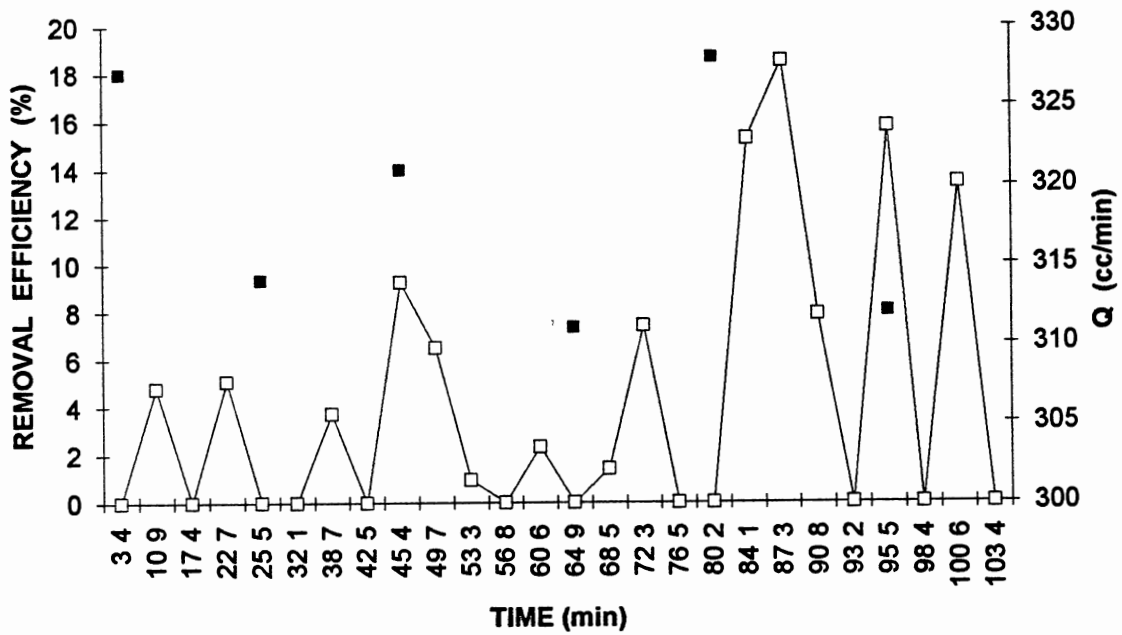


Figure 16. Results of Experiment 14. Conc. = 21.6 ppm C_6H_6 , Relative Humidity = 60.0%.

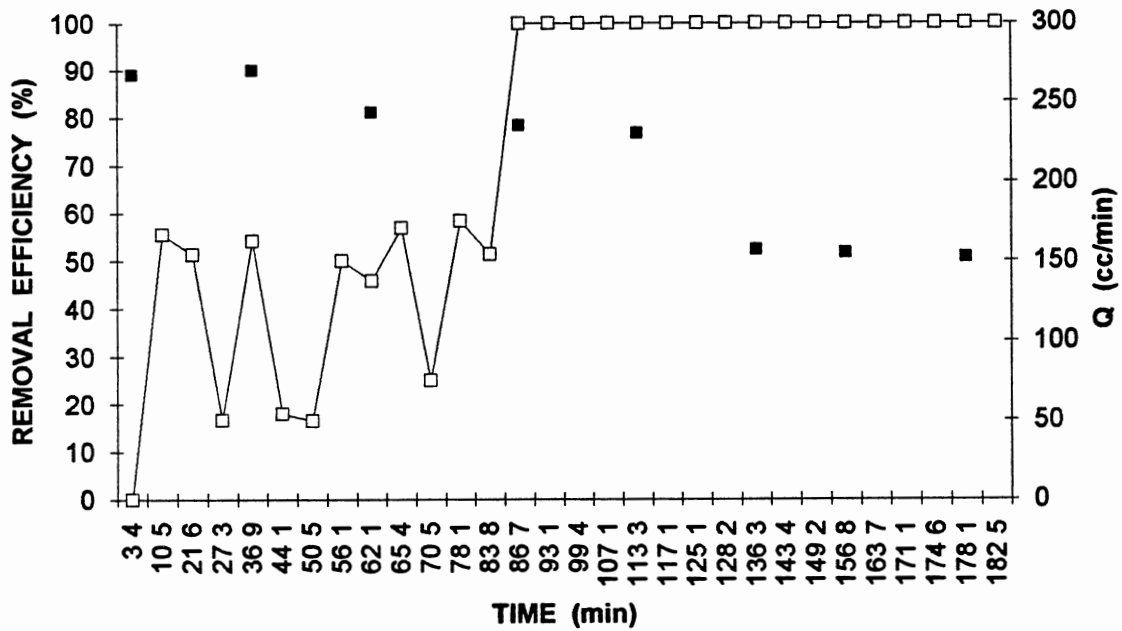


Figure 17. Results of Experiments 15 & 15A. Exp. 15: Conc= 7.2 ppm C_6H_6 , Humidity = 23.5%. Exp. 15A: @ 136 min. Q_R change & Conc.= 6.4 ppm, Relative Humidity = 21.0%.

The experimental process was designed to determine removal efficiency of influent pollutant streams of benzene when exposed to a photocatalytic reactor. This however, did not include mass spectrometry or other analytical measurements to determine what reaction products were produced as a result of the photocatalytic process. Furthermore, the extent to which photocatalytic processes versus adsorptive forces of the titanium/silica surface are responsible for overall benzene removal can only be estimated. This estimation is based on the results of the two additional experiments, #16 & #17.

The initial 60 minutes of experiment #16 (Figure 18), were conducted without the influence of ultraviolet irradiation. A minimal amount of benzene removal is experienced during this "dark" period of the experiment. Once the ultraviolet light is turned on (61 min.), 100 percent conversion of this dilute (8 ppm), low humidity influent stream is established in approximately 30 minutes. A steady-state conversion efficiency of 100 percent continued for the next 45 minutes. At 136 minutes the ultraviolet light was once again turned off. The removal efficiency of the reactor however, continued to be 100 percent for the next 20 minutes. At 189 minutes the benzene is no longer removed as influent concentrations equal reactor effluent concentrations. At this point the benzene influent is turned off. A relatively dry air stream (23% R.H.), is flowed through the reactor over the next 11

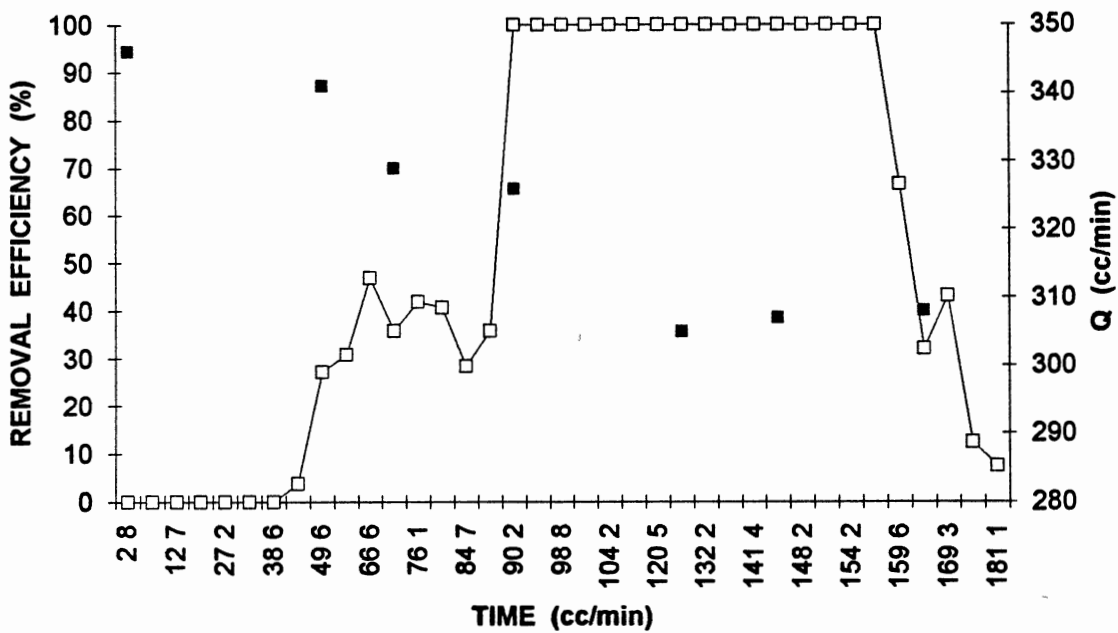


Figure 18. Results of Experiment 16. Initial 60 minutes = "dark period." Conc. = 8.1 ppm C_6H_6 , Rel. Humidity = 24%. AT 61 min. UV light turned on. At 104 min. turn UV off. AT 189 min. turn off C_6H_6 .

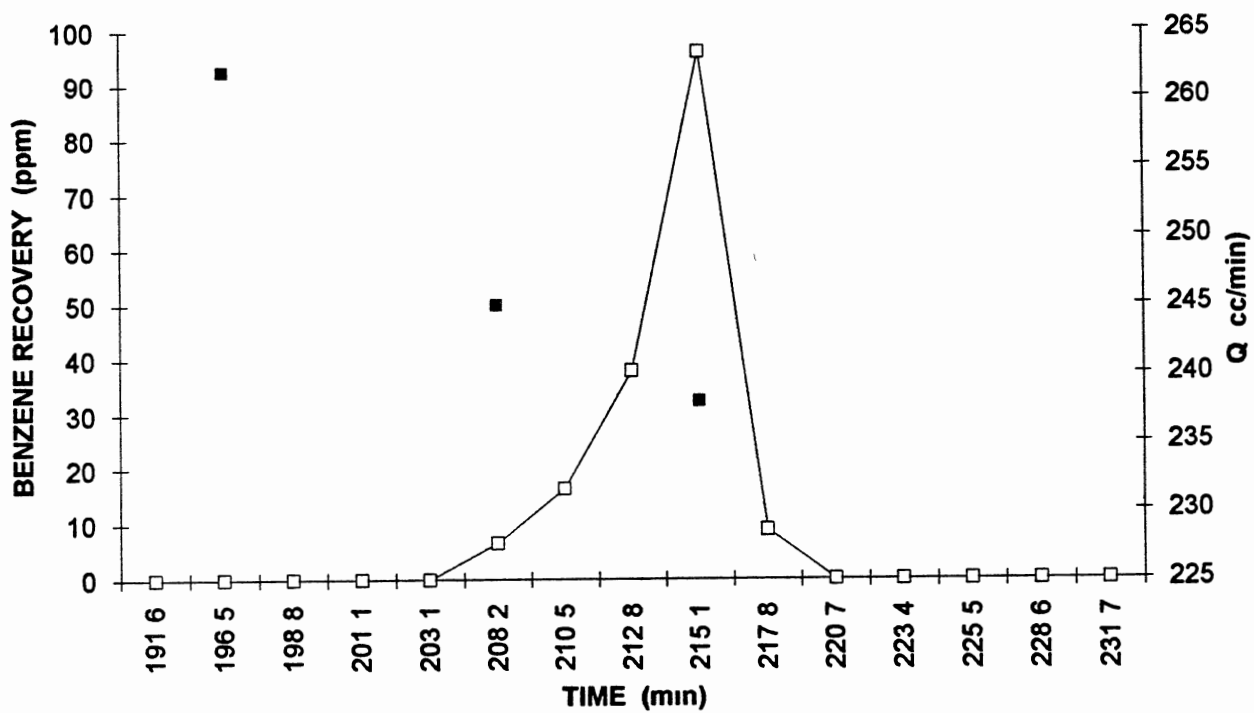


Figure 19. Continuation of Exp. 16. At 189 min.- Air Stream @ Relative Humidity = 23%. At 206 min. change to Humid Air @ 79% R.H.

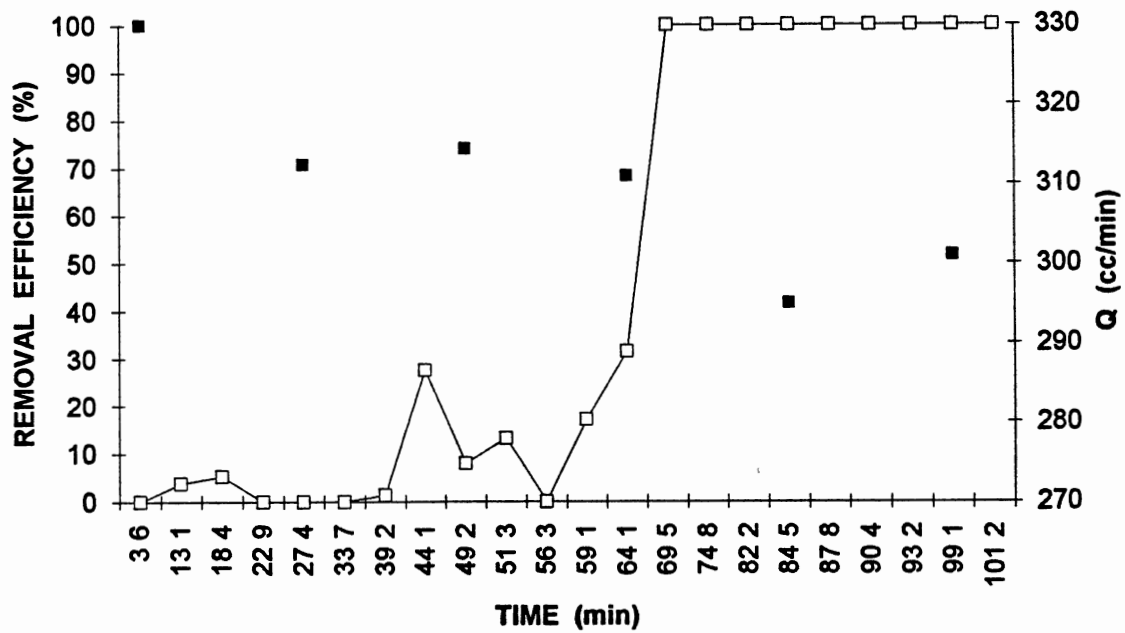


Figure 20. Results of Experiment 17. Conc.= 7.6 ppm C_6H_6 , Rel. Humidity = 25.0%. At 102 min. C_6H_6 & UV light turned off.

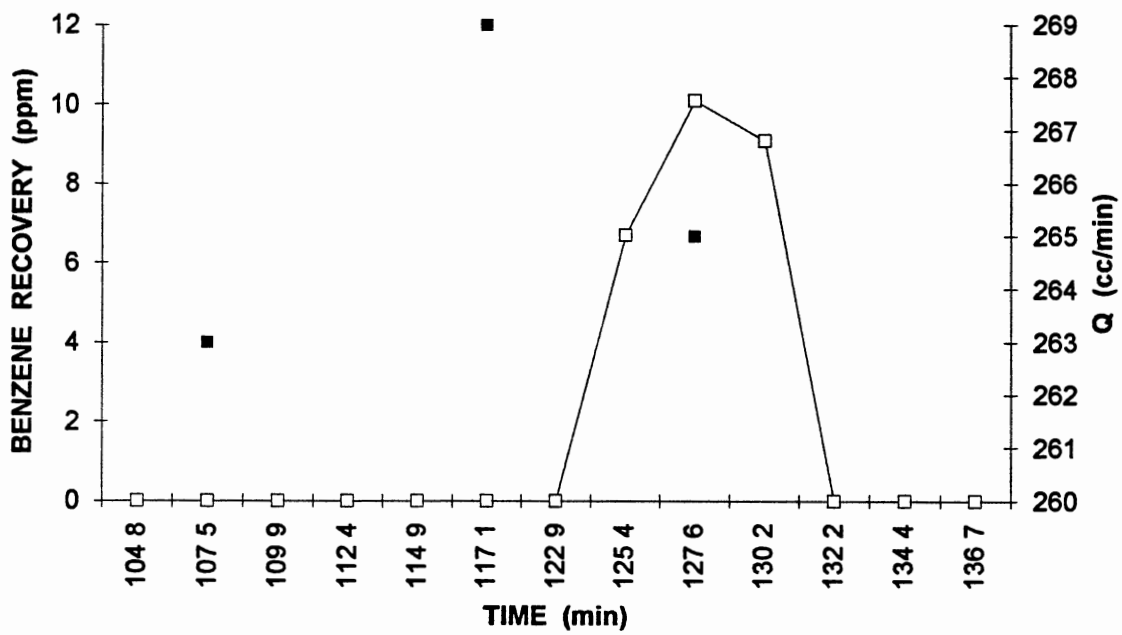


Figure 21. Continuation of Experiment 17. At 102 min. Air Stream @ Rel. Humidity = 24.5%. At 122 min. change to Humid Air @ 85% R.H.

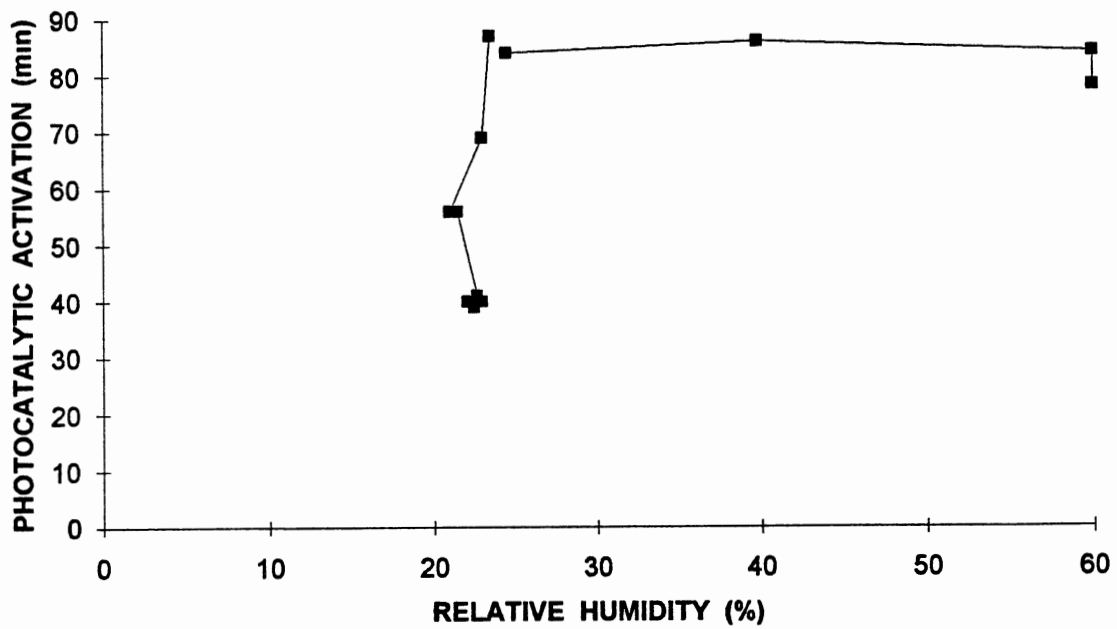


Figure 22. Photocatalytic Activation Time vs. Relative Humidity. All data represents "fresh-bed" experiments.

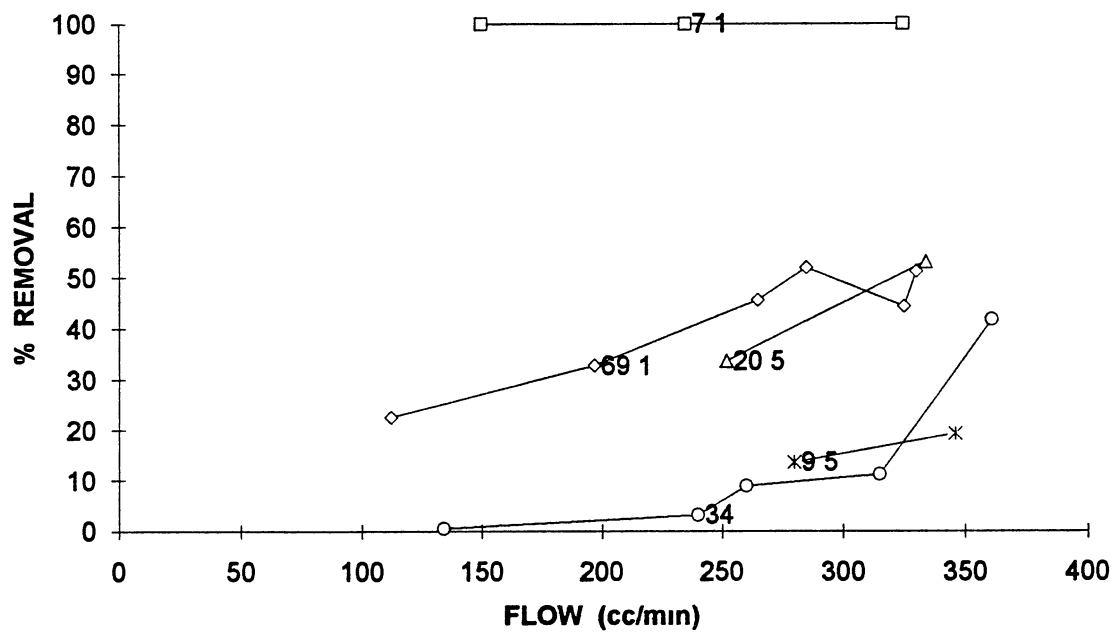


Figure 23. Removal Efficiency vs. Q_R . Concentrations as listed represent the average value of each line's data.

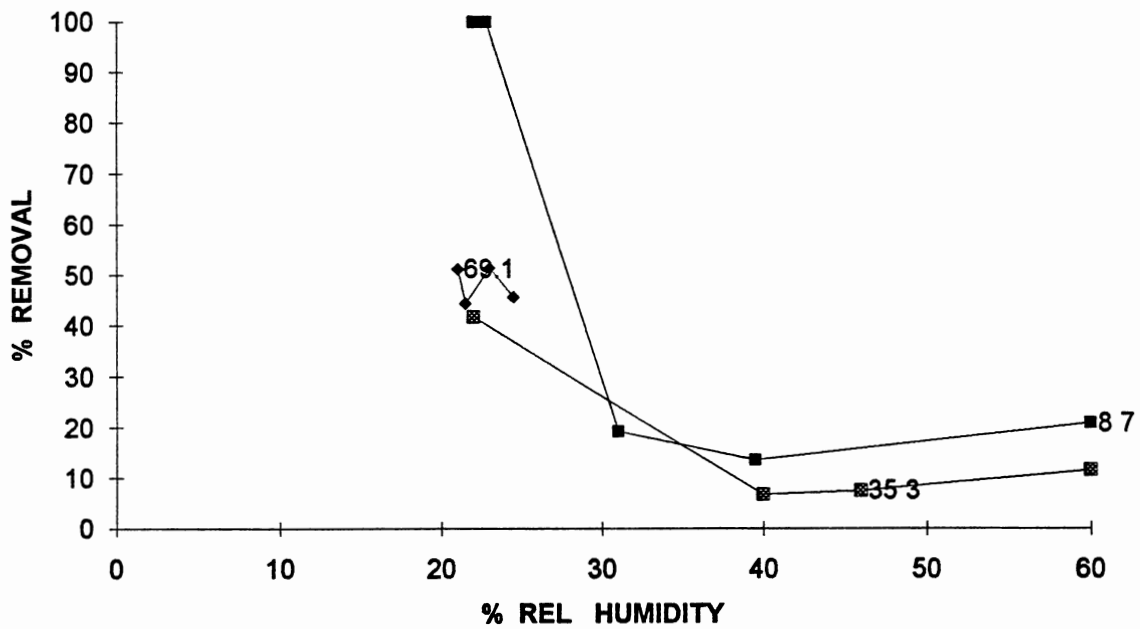


Figure 24. Removal Efficiency vs. Relative Humidity
 Concentrations listed represent the average value of
 each lines data.

Figure 24. illustrates the effect changes in the stream's relative humidity has on overall removal efficiencies under various concentrations. Data trend lines are based on experimental runs of similar volumetric flow and concentration ranges. Figure 24. shows that a reduction in removal efficiency can be expected if humidity is increased above 24 percent. Removal efficiency is vastly reduced as relative humidities of influent streams approach 30 percent, but seem to rebound slightly when relative humidity tops 40 percent. Experimental limitations prevented high concentration runs of 69 ppm to be performed under relative humidities greater than 24 percent. Thus no trend can be established for the 69.1 ppm data line plotted in Figure 24. Figures 23. and 24. dictate that the highest removal efficiencies can be expected in low humidity, low concentration influent streams.

Figure 25. represents a plot of steady state global reaction rates R_g , vs. influent stream concentration. The experimental results plotted in this figure were limited to runs in which flows exceeded 320 cc/min and relative humidities were less than or equal to 22.5 percent. A definite downward trend in global reaction rates is established as concentration is lowered.

In Figure 26. R_g is plotted vs. relative humidity. All data points are representative of results for experiments in which flow is greater than or equal to 200 cc/min and concentration is ≤ 40 ppm. Once again a clear

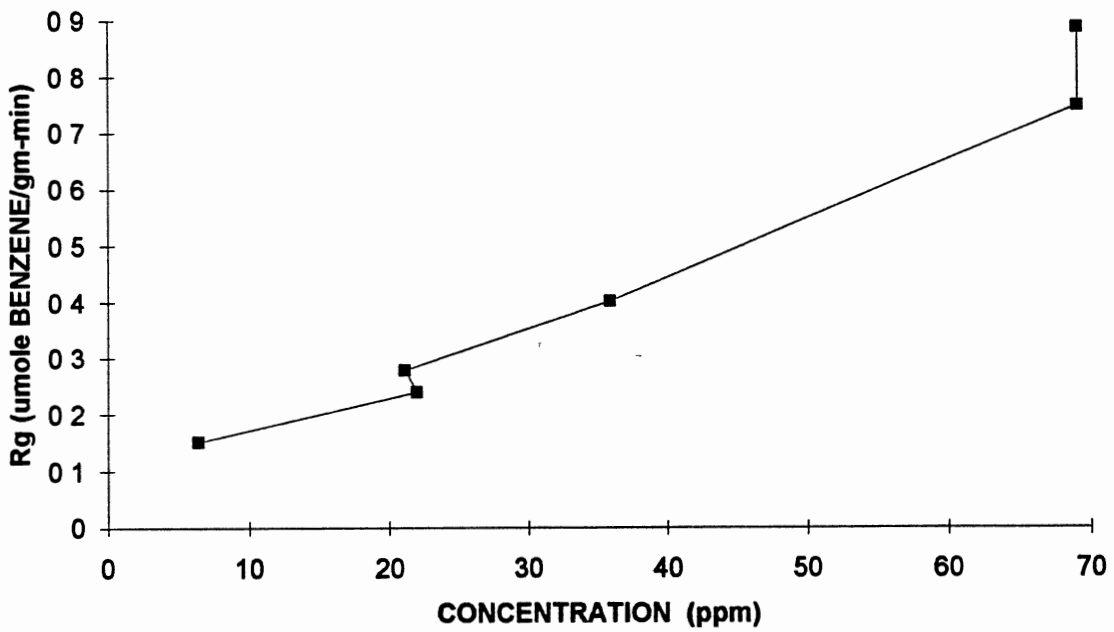


Figure 25. R_G vs. Concentration. $Q_R \geq 320 \text{ cm}^3/\text{min}$ for all data plotted. Relative Humidity $\geq 22.5\%$ for all data plotted.

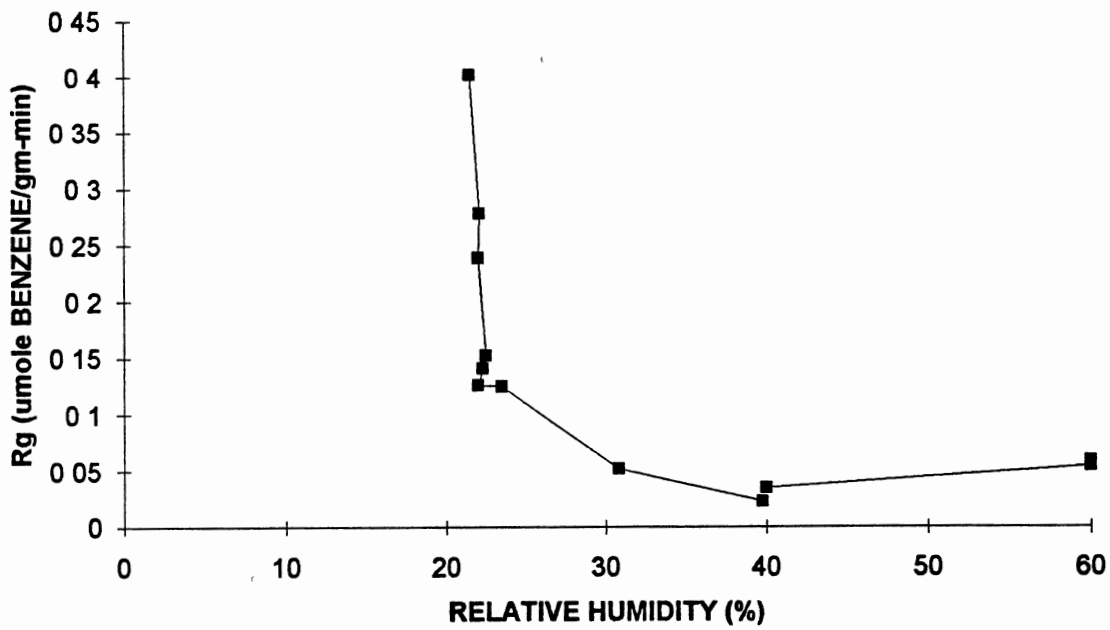


Figure 26. R_g vs. Rel. Humidity. $Q_R \geq 200 \text{ cm}^3/\text{min}$.
 Conc. $\leq 40 \text{ ppm C}_6\text{H}_6$.

trend is established as humidity exceeds 24 percent, as a decrease in R_g is noted as relative humidity is increased. These patterns are similar to those established in the overall removal efficiency plots.

Figure 27. illustrates the effect flow has on the global reaction rates. A definite downward trend is evident as volumetric flow rates are decreased in both concentrations ranges plotted. The overall depressed reaction rate for low concentration species is clearly depicted in Figure 27. Relative humidities of both data series were in the range of 22 to 24 %.

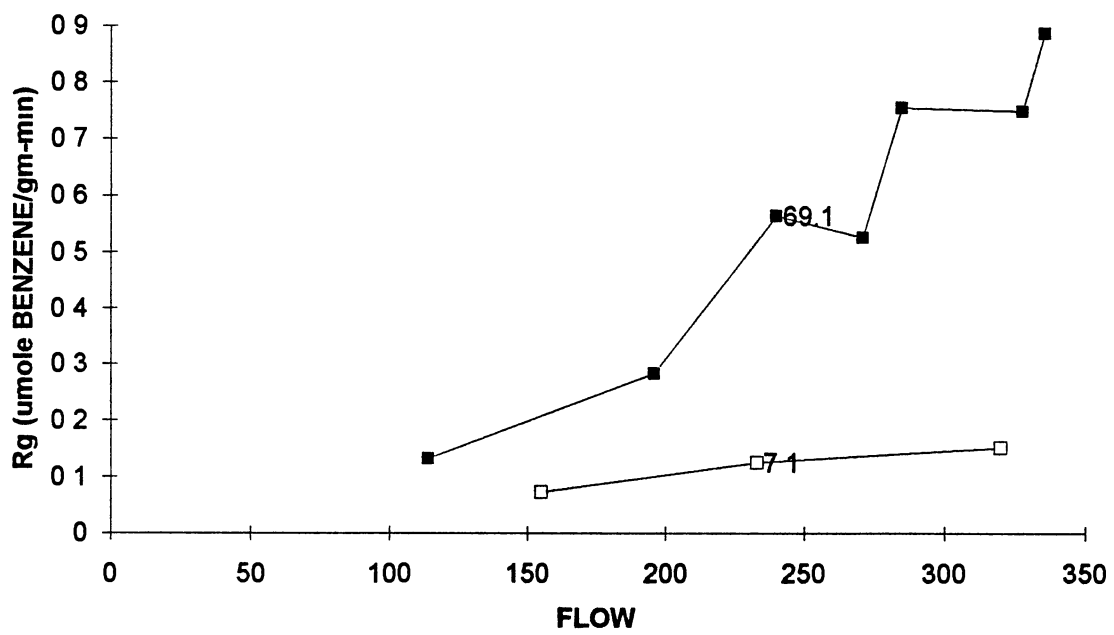


Figure 27. R_G vs. Q_R . Relative Humidities @ 22 - 24%

CHAPTER V

SUMMARY AND RECOMMENDATIONS

The removal of dilute gaseous benzene streams under ambient conditions has been accomplished in this research with varying degrees of success. This work shows that complete removal of low concentration (≤ 10 ppm), low relative humidity ($\leq 24\%$) benzene streams can be achieved over a wide range of influent flow regimes using a silica-supported titanium dioxide fluidized bed reactor under the influence of near ultraviolet irradiation.

Reaction rates as high as 0.88 umoles benzene/gm-min of total reactor catalyst bed were accomplished with volumetric flowrates > 300 cm³/min. This compares to reaction rates of 0.8 umoles TCE/gm-min at 248 cm³/min attained under similar experimental methods performed by Dibble (1989), in which TCE was used as the reactant stream. The fact that our reactor was able to attain higher reaction rates at higher flows may be accounted for by a combination of various factors. The first of these revolves around the makeup of the catalyst. Dibble's catalyst bed consisted of 0.632 grams of TiO₂ per gram of silica, where as the catalyst used in this research consisted of 3.269 grams of TiO₂ per gram of silica. Based on previous research of aqueous and gaseous phase aromatics, a more difficult destruction scenario was expected using benzene as opposed

to a chlorinated alkene such as TCE. Thus a catalyst bed containing a higher titanium constituent was employed.

The flow characteristics of the reactor may have also contributed to the favorable results of our experiments. Dibble reported difficulty in achieving good fluidization throughout the reactor due to a lack of porosity in the glass frit located above the reactor inlet line. Thus the entire reactor catalyst bed could not actively participate in the reaction process due to various stagnant or "plugged" regions. Conversely the reactor used in this research showed little evidence of any such plugged zones, thereby allowing high levels of fluidization at flows > 250 cc/min.

Although the specific reaction mechanisms for the removal process was not determined, an extensive literature review of similar research suggests that a heterogeneous photocatalytic reaction mechanism could be responsible for the complete oxidation of the influent reactant benzene stream. This reaction process assumes the benzene molecules are photo-reduced on the catalyst surface via photo-produced radicals (most likely HO^\cdot , HO_2^\cdot). This process evolves in response to excitation of the electrons in the semiconductor (TiO_2) by a photon of the appropriate energy level.

This research also showed that untreated "fresh" catalyst beds require a certain amount of initial conditioning time (approx. 60 min.), before photocatalytic reactions become consistently steady-state in nature. Dibble likewise experienced this transient period and

equated this time to a period necessary for the establishment of reactant, oxygen, and water photoadsorption equilibrium (Dibble 1989, page 151).

The effects of influent concentration, relative humidity and volumetric flowrate on reactor performance have been explored extensively in this paper. Deactivation of most catalytic reactions occur when relative humidities of 30% or more are encountered. Volumetric flowrates must be high enough to assure fluidized bed characteristics, thus preventing short-circuiting or inefficient use of the charged catalyst bed. Flow rates of less than 250 cc/min proved to be ineffective for benzene removal (except under dilute conditions of ≤ 10 ppm.)

At high influent benzene concentrations, higher reaction rates were experienced. However, removal efficiencies showed no direct relationship in regards to influent reactant stream concentrations. The best results could be expected ≤ 10 ppm, with varied results between 20 - 60 ppm.

Recommendations

This study has laid the ground work for continued study which is necessary to assess the feasibility of fluidized-bed photocatalytic systems for contaminated air stripping applications. The following recommendations include specific examples of areas in which work could be completed in order to enhance the findings of this research.

1. Determine the reaction end products in order to better quantify the chemical transformations which may evolve.
2. Perform long-term uninterrupted experiments in order to assess titanium dioxide bed life capabilities and rates of deactivation.
3. Experiment with different light intensities. Determine if reaction rates develop in a linear fashion in response to light intensity.
4. Investigate the application of this reactor with different compounds or mixtures which could be expected in a typical contaminated air stripping facility.

REFERENCES

- Boonstra, A.H., & Mustsaers, C. A. (1979). Redox catalysis in water cleavage. Journal of Physical Chemistry, 79, pg. 2025.
- Dibble, L.A. (1989), "Gas-Solid heterogeneous photocatalytic oxidation of trichloroethylene by near ultraviolet illuminated titanium dioxide." Thesis, Arizona State University.
- Dibble, L.A., & Raupp, G.B. (1992). Fluidized bed photocatalytic oxidation of trichloroethylene in contaminated airstreams. Environmental Science & Technology, 26(3), 492-495.
- D'Oliveira, J.C., Al-Sayyed, G., & Pichat, P. (1990). Photodegradation of 2- and 3- chlorophenol in titanium dioxide aqueous suspensions. Environmental Science & Technology, 24(7), 990-995.
- Duonghong, D., Borgarello, E., & Gratzel, M. (1981). Dynamics of light-induced water cleavage in colloidal systems. Journal of the American Chemical Society, 103(16), 4685-4687.
- Fire, F.L. (1988). Benzene: Chemical data notebook series #29. Fire Engineering, 141(10), 77-80.
- Formenti, M.F., Meriaudeau, J.P., & Teichner, S.J. (1971). Heterogeneous photocatalysis for partial oxidation of paraffins. Chemical Technology, 1(11), 680-686.
- Fujihira, M., Satoh, Y., & Osa, T. (1981). Heterogeneous photocatalytic oxidation of aromatic compounds on titanium dioxide. Nature, 293(17), 206-207.
- Gab, S., Schmitzer, J. Thamm, H.W., Parlar, H., & Korte, F. (1977). Photomineralisation rate of organic compounds adsorbed on particulate matter. Nature, 270(24), 331-333.
- Gerischer, H. (1985). Photochemistry, Photocatalysis, and Photoreactors. Schiavello, M. Ed. Reidel Publishing Company, Holland.

- Hadley, P.W., & Armstrong, R. (1991), Where's the benzene?- Examining California ground-water quality surveys. Ground Water, 29(1), 35-39.
- Izumi, I., Dunn, W.W., Wilbourn, K.O., & Baro, A.J. (1980). Heterogeneous photocatalytic oxidation of hydrocarbons on platinized titanium dioxide powders. Journal of Physical Chemistry. 84(24), 3207-3210.
- Kormann, C., Bahnemann, D.W., & Hoffman, M.R. (1991). Photolysis of chloroform and other organic molecules in aqueous titanium dioxide suspensions. Environmental Science & Technology, 25(3), 494-500.
- Marusk, H.P., & Ghosh, A. K. (1978). Photocatalytic decomposition of water at semiconductor electrodes. Solar Energy, 20(3), 443-458.
- McCarty, P.L. (1983), "Control of Organic Substances in Water & Wastes Water." EPA-600/8-83-001/, B.B. Berger, editor. U.S. EPA. Office of Research and Development, Cincinnati, Ohio. April, 1983.
- McGaughy, J.F., Much, M.L., & Ackerman, P.L. (1984). "Assessment of Treatment Products from Disposed Hazardous Waste Listings." EPA-68-02-3148. U.S. EPA Waste Treatment Branch, Cincinnati, Ohio. 1984.
- Miltner, R.J. & Love, O.T. (1984). " A comparison of procedures to determine adsorption capacity of VOC's on Activated Carbon." AWWA Water Quality Technology Conference Proceedings. Denver, Colorado, December 1984.
- Mozzanega, M., Herrman, J.M., & Picat, P. (1977). Oxydation D'lkytoluenes en alkylbenzaldehydes au contact de titanium dioxide irradié sous uv. Tetrahedron Letters, 34, 2965-2966.
- Neely, W.B., & Blau, G.E., (1984). Environmental Exposure From Chemicals. Volume I. CRC Press Inc., Boca Raton, Florida. page 176.
- Pelizzetti, E. (1983). Energy Resources Through Photochemistry & Catalysis. Academic Press, New York.
- Pichat, P., Hermann J. M., & Mozzanega, M. N. (1982). Photocatalytic oxidation of various compounds over titanium dioxide and other semiconductor oxides. THE Canadian Journal of Chemical Engineering, 60(2), 27-32.

- Pruden, A. L., & Ollis, D. F. (1983). Degradation of chloroform by photoassisted heterogeneous catalysis dilute aqueous suspensions of titanium dioxide. Environmental Science and Technology, 17(10), 628-631.
- Radford B., & Francis, J. (1983). Semiconductor properties of titanium dioxide. Journal of the American Chemical Society Communications, 1520.
- Roy, K. A. (1991). Casting a new light - Uv system breaks down organics in air, soil, and water. Hazmat World, December, 1991. pp. 32-35.
- Seeger, D. R., Slocum, C. J. & Steen, A. A. (1978). "GC/MS analysis of purgable contaminants in source and finished drinking waters." in EPA document /625/4-85/016. pp. 157-175.
- Shearman, J. (1992) Benzene: balancing supply and demand. Chemical Engineering, 99(4), 63-64.
- Sutton, M. M., & Hunter, E. N. (1985). Solar destruction of Hazardous Organic Wastes. Pollution Engineering, October, 1985. pp. 86-89.
- Wiseman, T. J. (1976). Characterization of Powder Surfaces. G. D. Parfitt and K. S. W. Sird eds. Academic Press, New York, 1976. pp. 159-160.

VITA

Lawrence J. DeFluri

Candidate for the Degree of

Master of Science

Thesis: HETEROGENEOUS PHOTOCATALYTIC REMOVAL OF GASEOUS
DILUTE BENZENE STREAMS VIA NEAR ULTRAVIOLET
ILLUMINATED TITANIUM DIOXIDE

Major Field: Environmental Engineering

Biographical:

Personal Data: Born in Hazelton, Pennsylvania,
November 7, 1964, the son of Neil and Nancy
DeFluri.

Education: Graduated from Parkland High School,
Orefield, PA., in June 1982; received B. S.
in Petroleum and Natural Gas Engineering from
The Pennsylvania State University in August 1986;
completed requirements for Master of Science
degree at Oklahoma State University in December,
1992.

Professional Experience: Petroleum Engineer, Tenneco
Oil Exploration & Production Company 1986 - 1987,
Project Engineer, Martin Bradbury & Griffith Inc,
Allentown, PA., 1988 - 1990; Project Environmental
Engineer, R.E. Wright Associates, Middletown, PA.,
November 1992 - present.